Title
Understanding memristors and memcapacitors in engineering mechanics applications

Journal
Nonlinear Dynamics, 80(1-2)

ISSN
0924-090X

Authors
Pei, Jin-Song
Wright, Joseph P
Todd, Michael D
et al.

Publication Date
2015-04-01

DOI
10.1007/s11071-014-1882-3

Peer reviewed

Noname manuscript No.
(will be inserted by the editor)

Understanding memristors and memcapacitors in engineering mechanics applications

Jin-Song Pei · Joseph P. Wright · Michael D. Todd · Sami F. Masri · François Gay-Balmaz

Received: date / Accepted: date

Abstract A significant event happened for electrical engineering in 2008, when researchers at HP Labs announced they had found "the missing memristor", a fourth basic circuit element that was postulated nearly four decades earlier by Dr. Leon Chua, who was also instrumental in developing the mathematical theories of memristive, memcapacitive and meminductive systems, resulting in an entire class of "mem-models" that are the foundation of the present work. By applying well-known mechanical-electrical analogies, the mathematics of mem-models may be transferred to the setting of engineering mechanics, creating the mechanical counterparts of memristors, memcapacitors, etc. However this transfer is nontrivial; for example, a new concept and state variable called "absement", the time integral of deformation, emerges. We study these mem-models, which are characterized by a "zero-crossing" property that has interesting implications for nonlinear constitutive modeling, particularly hysteresis, and we identify some examples of "mem-dashpots" and "mem-springs", which include displacement-dependent and variable dampers, the superelasticity found in shape memory alloys, and the pinched hysteresis loops associated with self-centering structures. This work adds to the fast-growing body of literature on elements and systems labeled with "mem", which is a basic branch of study in nonlinear dynamics.

Keywords Nonlinear hysteresis · memristor · memcapacitor · memristive system · memcapacitive system · state equation · input-output equation · displacement-dependent damper · variable damper · flag-shaped hysteresis · shape-memory alloy · self-centering structure

Jin-Song Pei
School of Civil Engineering and Environmental Science
University of Oklahoma
Norman, Oklahoma 73019-1024
Tel.: +1-405-325-4272
Fax: +1-405-325-4217
E-mail: jspei@ou.edu

Joseph P. Wright
Division of Applied Science
Weidlinger Associates Inc.
New York, NY 10005

Michael D. Todd
Department of Structural Engineering
University of California, San Diego
9500 Gilman Drive, Mail Code 0085
La Jolla, CA 92093

Sami F. Masri
Sonny Astani Department of
Civil and Environmental Engineering
University of Southern California
Los Angeles, CA 90089-2531

François Gay-Balmaz
CNRS Researcher
Laboratoire de météorologie dynamique
Ecole Normale Supérieure
24 Rue Lhomond
75005 Paris, France

1 INTRODUCTION

1.1 Motivations of This Study

Modeling hysteresis (e.g., Sozen (1974); Visintin (1994); Nayfeh and Mook (1995); Sivaselvan and Reinhorn (2000); Farrar et al (2007); Bernstein (2009)) is inherently challenging; however, it is necessary in that it has broad utility in many engineering disciplines, including smart structures, robotics, mechatronics, structural control, structural health monitoring, damage detection, and earthquake engineering. Rapid advances in sensor technology are providing researchers in different fields of science and engineering with valuable data collected from real-world measurements. Facing formidably large streams of such data, researchers are expected to extract the most useful and accurate information to enable rapid assessment for decision-making, and modeling plays a central role. This study explores one possibility for very generally modeling hysteresis, adopted from another discipline.

Development of a fundamental circuit element, the memristor, was announced recently (Strukov et al (2008)), nearly four decades after its prediction (Chua (1971)). Equally important, there is a mathematical theory involving memristor devices and memrisitive systems (Chua and Kang (1976)) and, more recently, this theory was extended to include memcapacitors and meminductors (Di Ventra et al (2009)), thereby significantly enlarging this family of "mem-models". These developments have inspired us to explore whether these nonlinear constitutive models, all of which are characterized by a "zero-crossing" property, have a role to play in engineering mechanics.

Two obvious but related conceptual gaps need to be bridged first in this study: from electronics to mechanics, and from nano- to macro-scale modeling. Bridging these gaps is made possible, in part, by applying mechanical-electrical system analogies. Bond graph theory (Paynter (1961); Rosenberg and Karnopp (1983)) also helps to bridge the gaps. Starting from these well-established techniques, we identify the mechanical counterparts of the memristor, memcapacitor, memrisitive systems, etc., and identify some examples of these mem-models found in recent engineering mechanics literature.

The transfer from one knowledge domain to another is not straightforward. The mem-models defined in Chua (1971); Chua and Kang (1976); Di Ventra et al (2009) are mathematically abstract, demanding significant effort to translate the terminology and mathematical notation from electrical systems theory to other physical domains. Also, many functional forms need to be examined in order to develop mem-models usable in practical data analysis and modeling. Georgiou et al (2012) is one of the few recent studies with specificity in functional form; however, it covers a relatively simple situation, and is not from the field of engineering mechanics. Jeltsema and Dòria-Cerezo (2010) discuss difficulties that may arise when introducing mem-models in classical Lagrangian or Hamiltonian mechanics and propose a "port-Hamiltonian" approach as a way to overcome these difficulties. Other references are cited in the literature review (Section 2) and in subsequent sections, but generally speaking, there are very few published studies relevant to the engineering mechanics community. This is mainly because these mem-models are so "new", even though the physical and mathematical basis of memristors was first presented many years ago. We are thus motivated to investigate these models and to examine their potential for dealing with engineering mechanics problems.

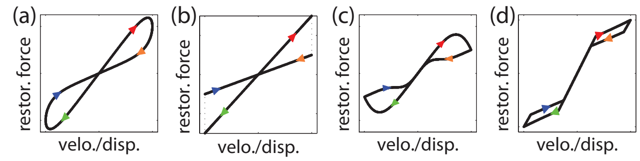

Fig. 1 (a) to (d) are from simulations using memristors/memcapacitors subject to cyclic or sinusoidal loading; see Figs. 10(a), 11(b), 27(b), and 9, respectively.

As a preview, consider a single-degree-of-freedom (SDOF) model:

$$m\ddot{x}(t) = u(t) - r(t) \tag{1}$$

where $x(t)$ is the displacement of mass m, $u(t)$ is its driving force, $r(t)$ is its restoring force, and

$$r(t) = c\dot{x}(t) + kx(t), \text{ for a linear dashpot and spring} \tag{2}$$

$$r(t) = M(x)\dot{x}, \text{ for a memristor} \tag{3}$$

$$r(t) = M(a)x, \text{ for a memcapacitor} \tag{4}$$

The restoring force in Eq. (2) is widely studied and understood, whereas the nonlinear damper in Eq. (3) is not so well known, and certainly not by the name "memristor". In Eq. (4), $a(t)$ is the integral of $x(t)$ with respect to time; we are unaware of any such "memcapacitor" in engineering mechanics. Eqs. (3) and (4) are the simplest examples of mem-models to be studied herein. Fig. 1 presents four pinched hysteresis loops, taken from computational results that will be discussed later. It is worth noting that the abscissa of each panel in Fig. 1 has two labels, velocity or displacement, due to the fact that Equations (3) and (4) have identical mathematical form, although the physical units of the function $M(\cdot)$ differ.

1.2 Contributions and Structure of This Paper

This paper demonstrates the usefulness of memristive and memcapacitive theories for modeling some important nonlinear hysteretic systems in engineering mechanics. Specifically, displacement-dependent and variable dampers are memristive systems. Also, the superelasticity of shape-memory alloys (SMA) and the pinched hystersis of self-centering structures may be modeled as memcapactive systems, a premise justified (in part) by devising and presenting quantitative mem-models using simulations and experimental data in Section 5. This paper also connects mem-models with broader classes of constitutive models in engineering mechanics in Section 5.4 and Section 6, thereby highlighting future research directions.

The Literature Review in Section 2 summarizes basic concepts and translates mem-model theories from electrical engineering to engineering mechanics. Mem-dampers and mem-springs are formally introduced in Section 3. Due to their newness, mem-springs subjected to two typical kinds of periodic inputs are the main focus when deriving various properties. These properties not only illuminate understanding but are also instrumental in modeling. Significant portions of this paper focus on detailed case studies, presented in Sections 4 and 5. Because mem-models are nonlinear (and thus lack many linear system properties and simplicity), such case studies are both necessary and enlightening. Moreover, we must pay attention to time and state events which arise in the case studies, where time events are the discontinuities inherent in nearly all excitation signals, and state events are the discontinuities inherent in a model's state variables. Regarding modeling technique, Section 4.6 outlines an approach, involving time-varying secants, which was first tested on mem-dashpot models, and later utilized to devise the quantitative mem-spring models discussed in Section 5.

In this paper, a Remark gives a brief review of existing knowledge. A Property presents useful results, put forth in detail for the first time in this study, and derived mainly for mem-models subjected to two classes of periodic excitation. Finally, an Example augments the case studies, providing specific mathematical expressions or numerical results of mem-model simulations.

2 LITERATURE REVIEW

2.1 Memristors, Bond Graphs and Physical Analogies

Chua's seminal memristor paper is Chua (1971). Two years later, Oster and Auslander (1973) proposed the memristor as a new bond graph element by interpreting Chua's idea in the context of Paynter's tetrahedron of state (Paynter (1961)) and using the Force-Current Analogy to explain a mechanical device called a "tapered dashpot". As told by Paynter (Paytner (2000)), bond graphs were born in 1959 as a result of his training and experience in hydroelectric power, which greatly reinforced his awareness of physical analogies. Physically different systems that have the same mathematical model are called analogous systems (Ogata (2004)). In other words, analogous systems are expressed by the same set of algebraic, differential (or integro-differential) equations, but the specific physical meaning of each parameter or state variable is different. Analogies are available for many kinds of mechatronic (i.e., electromechanical) systems, including translational and rotational mechanical systems, fluid power systems, electrical power systems, and heat transfer systems (Hogan and Breedveld (2002)). Today, bond graph models are routinely used when analyzing mechatronic systems with many degrees of freedom and, when appropriate, they incorporate finite element models (Talasila et al (2002); Damic and Cohodar (2006); Vaz and Maini (2009)). Another analogy – involving springs (capacitors), dashpots (resistors) and masses (inductors) – is the Force-Voltage Analogy (Ogata (2004)), which is applicable to translational mechanical systems and was used during this study (in addition to the Force-Current Analogy) to "translate" memristor theory and its extensions into mechanical notation and terminology; e.g., see Table 1. The Force-Current Analogy (Ogata (2004)) was also used.

Remark 1 (On p = Momentum or Impulse)

It is challenging to name p in Table 1 without a bit of thought. In classical mechanics, a particle's momentum is defined as the product of its mass and velocity, so in analytical mechanics p and q are called generalized momenta and generalized coordinates, respectively. This supports the naming of p and x as momentum and displacement, respectively, in engineering mechanics. It also supports the naming of p as momentum in Oster and Auslander (1973) or Jeltsema and Scherpen (2009) but there are reasons to support the naming of p as impulse (also mentioned in those two references). In classical mechanics, an impulse is defined as the time integral of force, resulting in a change of momentum, and thus impulse and momentum have the same physical units. No matter how we name p, the mathematical relationship between p and r is the same as between x and $\dot{x}$, in the sense that the first quantity is the time integral of the second. Paynter's tetrahedron of state includes both of these relationships.

Remark 2 (On r=restoring force)

The force r in Table 1 is not an applied (i.e., external) force. Rather, it is an internal force that characterizes a particular element (or system) in a constitutive equation. For example, for a spring or damper, r is a restoring force (Masri and Caughey (1979)); for a mass, r is its inertia force. An applied force is denoted in this paper by $u(t)$, as in Eq. (1).

2.2 Flow- and Effort-Controlled Systems

Bond graph practitioners distinguish a flow-controlled element (or system) from an effort-controlled element. Paynter's tetrahedron of state depicts relations among four state variables which, for electric circuit elements, are e = effort $= v =$ voltage, $f =$ flow $= i =$ current, $q =$ charge, $p =$ momentum $= \varphi = \phi =$ flux. These various symbols and terms are briefly mentioned here because they (and others) appear in Chua (1971), Oster and Auslander (1973) or Jeltsema and Scherpen (2009); see Table 8 in Appendix A. For electrical systems, charge- or current-controlled are aliases for flow-controlled, while flux-, voltage-, or impulse-controlled are aliases for effort-controlled. Thus when exercising the Force-Voltage Analogy, we see that Paynter's

Table 1 Force-Voltage Analogy used to translate from electrical to mechanical terminology.

	Electrical System	Translational Mechanical System
1.	Current i	Velocity $\dot{x}$
2.	Voltage v	Restoring force r
3.	Charge $q, dq = idt$	Displacement $x, dx = \dot{x}dt$
4.	Flux $\varphi, d\varphi = vdt \Longrightarrow \varphi = \int_{-\infty}^{t} v(\tau)d\tau$	Momentum $p, dp = rdt \Longrightarrow p = \int_{-\infty}^{t} r(\tau)d\tau$
5.	Resistor $dv = Rdi$	Dashpot $dr = cd\dot{x}$
6.	Capacitor $dq = Cdv$	Spring $dx = \frac{1}{k}dr$
7.	Inductor $d\varphi = Ldi \Longrightarrow v = L\frac{di}{dt}$	Mass $dp = md\dot{x} \Longrightarrow r = m\frac{d\dot{x}}{dt}$
8.	Memristor $d\varphi(q) = M(q)dq \Longrightarrow M(q) = \frac{v}{i}$ (Chua (1971))	Memristor $dp(x) = M(x)dx \Longrightarrow M(x) = \frac{r}{\dot{x}}$
9.	Memristor $dq(\varphi) = W(\varphi)d\varphi \Longrightarrow W(\varphi) = \frac{i}{v}$ (Chua (1971))	Memristor $dx(p) = W(p)dp \Longrightarrow W(p) = \frac{\dot{x}}{r}$
10.	$i - v$ for hysteresis (Chua (1971))	$\dot{x} - r$ for hysteresis
11.	$q - \varphi$ for additional insights (Chua (1971))	$x - p$ for additional insights

tetrahedron depicts relations among four state variables which govern translational mechanical elements: e = effort = r = restoring force, f = flow = $\dot{x}$ = velocity, x = displacement, and p = momentum. So for mechanical elements (or systems) under this analogy, displacement- or velocity-controlled are aliases for flow-controlled, while force- or momentum-controlled (or impulse-controlled) are aliases for effort-controlled.

As discussed in Rosenberg and Karnopp (1983), pages 20-21, flow (velocity) and effort (force) are called power variables because their product equals power, which is the time derivative of energy. Conversely, energy is the time integral of power. Momentum and displacement are called energy variables because instantaneous energy quantities (kinetic or potential) can be expressed naturally in terms of them. Displacement is the time integral of flow, while momentum is the time integral of effort. These four state variables (flow, effort, displacement, momentum), which are fundamental in power flow and energy conservation considerations for dynamical systems, are the vertices of Paynter's tetrahedron of state, regardless of the type of physical system of interest.

Loosely speaking, a flow-controlled system involves connecting two or more basic elements in parallel where the total kinetic quantities are summations of individual ones while all elements share the same kinematic quantities. In this case, the kinematic quantities need to be solved (or calculated) first. The contrary can be said about the kinetic quantities in an effort-controlled system where two or more basic elements are connected in series. An example is given in Appendix A; see Fig. 25 and corresponding equations in Table 9.

2.3 Mem-Elements and Mem-Systems

The constitutive equations for all mem-models (i.e., memristor, memcapacitor, meminductor, as well as memristive, memcapacitive and meminductive systems) are summarized in Table 2. Both the time-invariant elements and their time-varying systems definitions are included but hereafter we will restrict this study to time-invariant mem-models.

Remark 3 (On a = Absement and ρ)
The quantity a in Table 2 is the time integral of displacement x, while ρ is the time integral of momentum p. Although the name "absement" for a appears in Jeltsema (2012), it is not widely known or accepted. An online search uncovered "absition" as an alternative to absement. Another search uncovered "time integral of momentum" in Bellenger and Duvel (2009), but this article isn't about memcapacitors, and ρ wasn't given a name. Rather ρ was used to estimate an "average value" of the Diurnal Water Layer over the course of many days. This article is cited as an example of a study of time series data that might (eventually) lead to an engineering model of nonlinear behavior that is of interest in the field of meteorology.

Remark 4 (Passivity)
Chua (1971) provides necessary and sufficient conditions for a memristor (in isolation) to be passive such as $M(x) \geq 0$ for "any admissible input" $\dot{x}$ and output r for all time $t \geq t_0$. Similarly, Chua and Kang (1976) gives $M(\mathbf{y}, \dot{x}) \geq 0$ for time-invariant memristive systems, the generalization of memristors. However, this passivity condition is only sufficient if a memristor (element or system) is part of a more complicated system containing other elements that dissipate energy. (For example in the case of Fig. 25(2a), the weaker condition $M(x) \geq -c$ is sufficient for passivity of the combined system; see Appendix A.) Nonetheless, the passivity condition will be adopted in this paper, despite contrary considerations in Di Ventra and Pershin (2013). Together with Remark 9, the passivity condition restricts all memristor or memristive system paths to the first or third quadrants of the $(\dot{x}, r)$ plane.

Remark 5 (Mathematical Parallelism)
As was mentioned in the Introduction after Eq. (4), and as Table 2 shows, mem-models possess mathematical (i.e., functional) parallelisms that are noteworthy. However, physical units and energetics must also be considered; see Section 3.1. Also, see Table 10 in Appendix A for an example.

Table 2 Two forms of mem-models (element or system). All expressions were translated from Chua (1971); Oster and Auslander (1973); Chua and Kang (1976); Di Ventra et al (2009) by using mechanical-electrical system analogies. †$\mathbf{y}$ denotes a state variables vector, $\mathbf{g}$ and $\mathbf{f}$ denote vector functions, and M and W are scalar functions.

	Element or System	**Flow-Controlled**	**Effort-Controlled**
1.	Memristor (element)	$p = G(x)$ or $r = M(x)\dot{x}$	$x = F(p)$ or $\dot{x} = W(p)r$
2.	Memcapacitor (element)	$p = G(a)$ or $r = M(a)x$	$a = F(p)$ or $x = W(p)r$
3.	Memrinductor (element)	$\rho = G(x)$ or $p = M(x)\dot{x}$	$x = F(\rho)$ or $\dot{x} = W(\rho)p$
4.	Memristive System †	$\dot{\mathbf{y}} = \mathbf{g}(\mathbf{y}, \dot{x}, t)$ and $r = M(\mathbf{y}, \dot{x}, t)\,\dot{x}$	$\dot{\mathbf{y}} = \mathbf{f}(\mathbf{y}, r, t)$ and $\dot{x} = W(\mathbf{y}, r, t)\,r$
5.	Memcapacitive System †	$\dot{\mathbf{y}} = \mathbf{g}(\mathbf{y}, x, t)$ and $r = M(\mathbf{y}, x, t)\,x$	$\dot{\mathbf{y}} = \mathbf{f}(\mathbf{y}, r, t)$ and $x = W(\mathbf{y}, r, t)\,r$
6.	Meminductive System †	$\dot{\mathbf{y}} = \mathbf{g}(\mathbf{y}, \dot{x}, t)$ and $p = M(\mathbf{y}, \dot{x}, t)\,\dot{x}$	$\dot{\mathbf{y}} = \mathbf{f}(\mathbf{y}, p, t)$ and $\dot{x} = W(\mathbf{y}, p, t)\,p$

Remark 6 (On Invertibility)

The mathematical relationship between F and G in Table 2 and Table 8 is the same as for any basic element (electrical or mechanical) in the sense that one is the inverse of the other: $F^{-1} = G$ and $G^{-1} = F$. Also, W is the reciprocal of M (and vice versa) at any given point in time t.

Remark 7 (Reduction of Memristive System to Memristor)

Chua and Kang (1976) define memristive systems in terms of two equations, called the state equation and the input-output equation, from which the time-invariant version can be obtained. As a conceptual example of a flow-controlled memristive system, we have the following:

State Equation: $\dot{\mathbf{y}} = \mathbf{g}(\mathbf{y}, \dot{x}, t)$

$$\overset{\text{time inv.}}{\Longrightarrow} \dot{\mathbf{y}} = \mathbf{g}(\mathbf{y}, \dot{x}) \underset{\text{suff. conds. only}}{\overset{\text{for element: } \mathbf{y}=x}{\Longrightarrow}} \dot{x} = \dot{x} \tag{5}$$

Input-Output Equation: $r = M(\mathbf{y}, \dot{x}, t)\,\dot{x}$

$$\overset{\text{time inv.}}{\Longrightarrow} r = M(\mathbf{y}, \dot{x})\,\dot{x} \underset{\text{suff. conds. only}}{\overset{\text{for element: } \mathbf{y}=x}{\Longrightarrow}} r = M(x)\,\dot{x} \tag{6}$$

where $\mathbf{y}$ is the state vector, $\mathbf{g}$ is a vector function, and M is a scalar function. In this case, the velocity $\dot{x}$ is the input, while the restoring force r is the output. Trivial sufficient conditions for a time-invariant memristive system to reduce to a simple memristor are: $\mathbf{y} = x$, $\mathbf{g}(x, \dot{x}) = \dot{x}$, $M(x, \dot{x}) = M(x)$. These conditions are assumed in Eqs. (5) and (6). The final result in Eq. (6) is Eq. (3), which is a memristor, a subclass of memristive systems (as expected).

Remark 8 (Reduction of Memcapacitive System to Memcapacitor)

Di Ventra et al (2009) introduce another basic mem-model, a memcapacitive system in which a is the integral of displacement x with respect to time. As a conceptual example of a flow-controlled memcapacitive system, we have the following:

State Equation: $\dot{\mathbf{y}} = \mathbf{g}(\mathbf{y}, x, t)$

$$\overset{\text{time inv.}}{\Longrightarrow} \dot{\mathbf{y}} = \mathbf{g}(\mathbf{y}, x) \underset{\text{suff. conds. only}}{\overset{\text{for element: } \mathbf{y}=a}{\Longrightarrow}} x = x \tag{7}$$

Input-Output Equation: $r = M(\mathbf{y}, x, t)\,x$

$$\overset{\text{time inv.}}{\Longrightarrow} r = M(\mathbf{y}, x)\,x \underset{\text{suff. conds. only}}{\overset{\text{for element: } \mathbf{y}=a}{\Longrightarrow}} r = M(a)\,x \tag{8}$$

where $\mathbf{y}$ is the state vector, $\mathbf{g}$ is a vector function and M is a scalar function. In this case, the displacement x is the input, while the restoring force r is the output. Trivial sufficient conditions for a time-invariant memcapacitive system to reduce to a simple memcapacitor are: $\mathbf{y} = a$, $\mathbf{g}(a, x) = x$, $M(a, x) = M(a)$. These conditions are assumed in Eqs. (7) and (8). The final result in Eq. (8) is Eq. (4), which is a memcapacitor, a subclass of memcapacitive systems (again as expected). Another example is Eq. (15) in Di Ventra et al (2009).

Remark 9 (Zero-Crossing Property)

For a memristor, $r = 0$ when $\dot{x} = 0$ and vice versa. This means that the $(\dot{x}, r)$ intersection always goes through the origin, which is called the "zero-crossing" property in Chua and Kang (1976). In fact all mem-models in Table 2 have a zero-crossing property, determined by the corresponding pair of state variables in the input-output equation.

Remark 10 (On Nonlinearity)

It is important to note that the memristor is intrinsically nonlinear, not merely a classical resistor (constant), which is a linear time-invariant electrical engineering element; see page 511 of Chua (1971). By analogy, a classical viscous damper (constant) should not be considered a mechanical memristor, nor should a classical spring (constant) be called a mechanical memcapacitor.

3 PASSIVE MEM-SPRINGS AND MEM-DASHPOTS

3.1 Terminology and Scope of This Study

The point of departure for the rest of this paper is Table 2, which summarizes three classes of nonlinear constitutive equations where the elements in Lines 1-3 are subclasses of the corresponding systems in Lines 4-6. In the context of engineering mechanics, a classical dashpot model resists motion by means of a force that is directly proportional to velocity. By analogy and for brevity in this paper, memristors (elements) or memristive systems will often be called "mem-dashpots" because the ratio of resisting force to velocity is non-constant and explicitly depends on "memory" via the state vector $\mathbf{y}$. Similarly, the class of mem-models in

Lines 2 and 5 will often be called "mem-springs" because the ratio of restoring force to displacement is non-constant and explicitly depends on "memory" via the state vector $\mathbf{y}$, not simply on the current value of displacement. Hence as an example, the cubic term in the Duffing equation is not considered a mem-spring. The mem-models in Lines 3 and 6 will not be discussed further. Table 3 gives sample notation and physical units (see caption) that will be used as needed.

The scope of this study is limited to case studies of mem-springs and mem-dashpots in isolation, meaning not in combination with other elements (or systems). Moreover, thermodynamically passive mem-dashpots and mem-springs are of primary interest here. The focus is on discovering what the engineering mechanics literature holds regarding these two special mem-models. Due to their mathematical parallelism (Remark 5), insights gained about one should prove useful for the other. Therefore plots of force r versus velocity $\dot{x}$ and force r versus displacement x can be presented together (as in Fig. 1), despite the fact that mem-springs and mem-dashpots differ significantly in their physical interpretations, particularly their energetics.

Thus far, various passive mem-dashpot models have been found in the engineering mechanics literature but no unified studies, which simultaneously study passive mem-spring models have been found (although perhaps these appear, and other researchers will find them). Since their energetics are path-dependent, arrows that show increasing time have been added to the plots.

As noted in Remark 4, the passivity condition $D(\mathbf{y}, \dot{x}) \geq 0$ will be assumed for mem-dashpots, which along with the zero-crossing property restricts all paths in the ($\dot{x}$, r) plane to the first and third quadrants. Consequently, mem-dashpot power is never negative, and mem-dashpot energy cannot be created as time goes forward. In addition, the passivity condition $S(\mathbf{y}, \dot{x}) \geq 0$ will be assumed for mem-springs, which along with the zero-crossing property restricts all paths in the (x, r) plane to the first and third quadrants. Assuming the mem-spring displacement is zero at some point in time (sometimes called an initial or reference state), the amount of energy removed at any time thereafter cannot exceed the amount already stored up to that time; see the discussion pertaining to Fig. 3 in Di Ventra et al (2009).

The condition $D \geq 0$ alone suffices to prove that mem-dashpot models are passive whereas the parallel condition $S \geq 0$ is insufficient by itself to do the same for mem-springs. Clearly, it is more difficult to prove that mem-spring models (as a class) are passive, which presumably accounts for the lack of unified studies. This observation has motivated us to examine mem-spring models in more detail in subsections 3.3 and 3.4 , and to devise the quantitative mem-spring models presented in Section 5.

3.2 Examples of Mem-Dashpots

An example of a mem-dashpot is the "tapered dashpot" (Oster and Auslander (1973); Jeltsema and Scherpen (2009)). Table 11 in Appendix B summarizes other examples from the literature.

On the other hand, many commonly discussed types of damping are not mem-dashpots (memristors or memristive systems), such as linear viscous, air, Coulomb, displacement-squared, and solid or structural damping (e.g., Inman (1994)).

3.3 Mem-Springs $r = S(a)x$ Subject to Periodic Input

This subsection discusses several properties of mem-springs of the form $r = S(a)x$ subject to periodic input. The properties are illustrated via examples in Figures 3-8. Table 4 summarizes two different but related types of periodic input, displacement $x(t)$ and absement $a(t)$, plotted in Fig. 2. Table 12 in Appendix B gives the secant stiffnesses $S(a)$ and their differentiability classifications for all examples.

Due to mathematical parallellisms evident in Table 2, some of these mem-spring properties can be re-interpreted as properties of mem-dashpots of the form $r = D(x)\dot{x}$ by replacing x, a and S with $\dot{x}$, x and D respectively. Other useful results and insights can be obtained from these examples and properties by translating concepts, terminology and notation from flow-controlled elements to effort-controlled elements.

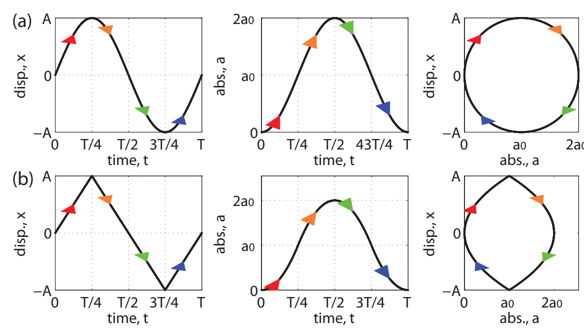

Fig. 2 Illustrations for (a) analytic, and (b) piecewise continuous displacement and absement defined in Table 4.

One type of periodic input is defined by a pair of analytic functions, Eqs. (9) and (10) in Table 4, where $A > 0$ is the amplitude of the sinusoidal displacement with period $T = \frac{2\pi}{\omega}$, and $a_0 = \frac{A}{\omega}$ is the value about which the analytic absement $a(t)$ oscillates. The related type of periodic input is defined by a pair of piecewise continuous functions, Eqs. (13) and (14) in Table 4. Eq. (13) is the piecewise linear ($\mathcal{C}^0$) displacement whose extrema coincide with the maxima and minima of the sinusoidal displacement. The related

Table 3 Two time-invariant flow-controlled mem-models. †$\mathbf{y}$ denotes a state variables vector, $\mathbf{g}$ denotes a vector function, and D and S are scalar functions bearing SI units of Newton · second / meter, and Newton / meter, respectively.

	Mem-Dashpots	Mem-Springs
State Eqs.	$\dot{\mathbf{y}} = \mathbf{g}(\mathbf{y}, \dot{x})$	$\dot{\mathbf{y}} = \mathbf{g}(\mathbf{y}, x)$
I/O Eq.	$r = D(\mathbf{y}, \dot{x})\dot{x}$	$r = S(\mathbf{y}, x)x$
Power	$P(t) = r(t)\dot{x}(t) \overset{\text{for element}}{=} D(x(t))\dot{x}^2(t)$	$P(t) = r(t)\dot{x}(t) \overset{\text{for element}}{=} S(a(t))x(t)\dot{x}(t)$
Energy	$U(t) = \int_0^t P(\tau)d\tau \overset{\text{for element}}{=} \int_0^t D(x(\tau))\dot{x}^2(\tau)d\tau$	$U(t) = \int_0^t P(\tau)d\tau \overset{\text{for element}}{=} \int_0^t S(a(\tau))x(\tau)\dot{x}(\tau)d\tau$

Table 4 The two related periodic motions (displacements and absements) used in Section 3.3.

Analytic Displacement and Absement	Piecewise Continuous Displacement and Absement
$x(t) = A\sin(\omega t)$ with $T = \frac{2\pi}{\omega}$ (9)	$x(t) = \frac{4A}{T}\left(t - \frac{T}{2}\left\lfloor \frac{2t}{T} + \frac{1}{2} \right\rfloor\right)(-1)^{\lfloor \frac{2t}{T} + \frac{1}{2} \rfloor}$ (13) where $\lfloor \cdot \rfloor$ denotes the floor function.
$a(t) = a_0(1 - \cos(\omega t))$ with (10)	$a(t) = a_0\left[1 \mp \left(1 - \frac{x^2}{A^2}\right)\right]$ with (14)
$a_0 = \frac{A}{\omega}$, $\bar{a} = a_0\sqrt{1 - \frac{1}{\omega^2}\frac{x^2(t)}{a_0^2}}$ (11)	$a_0 = \frac{\pi}{4}\frac{A}{\omega}$, $\bar{a} = a_0\left(1 - \frac{\pi^2}{16\omega^2}\frac{x^2}{a_0^2}\right)$ (15)
$\frac{da}{dx} = \frac{x}{\dot{x}} = \frac{A\sin(\omega t)}{A\omega\cos(\omega t)} = \frac{1}{\omega}\tan(\omega t)$ (12)	$\frac{da}{dx} = \frac{x}{\dot{x}} = t - \frac{T}{2}\left\lfloor \frac{2t}{T} + \frac{1}{2} \right\rfloor$ (16)

piecewise parabolic ($\mathcal{C}^1$) absement is the time integral of Eq. (13) with $a(0) = 0$ (consistent with the analytic absement). Hence a_0 for the related absement differs by a factor of $\frac{\pi}{4}$ from a_0 for the analytic absement. These quantities are defined for notational convenience and insight in analysis, and all examples are plotted with respect to A, ω, and a_0 as a way of "normalizing" and comparing results. In many figures, dissipated energy is indicated by a plus sign inside a clockwise hysteresis loop in the (x, r) plane, whereas stored (or created) energy is indicated by a minus sign inside a counter-clockwise loop.

Note that in certain situations when $t = 0, \frac{T}{4}, \frac{T}{2}, \frac{3T}{4}, T$, the corresponding values of $r(t)$ (or other variables) are not always unique, meaning one-sided limits must be considered at those times. Thus for notational convenience, the four quarter periods – called Phases 1,2,3 and 4 – are detailed in Eqs. (17) to (20) along with $\bar{a}(t)$ in Eqs. (11) and (15).

Property 1 (Asymmetry of Secant Stiffness $S(a)$ about a_0)
Under certain conditions, a mem-spring model can degenerate into a nonlinear (or even linear) spring without memory, meaning there is no hysteresis loop in the (x, r) plane. As an example, if $S(a)$ is an even function with respect to a_0 (i.e., $S(a_0 - \xi) = S(a_0 + \xi)$ for all ξ), such degeneracy happens, as Fig. 3 illustrates. Hence the remaining examples involve secant stiffnesses $S(a)$ which, by design, are not even functions about a_0.

Property 2 (Orientation of Hysteresis Loops)
If $S(a)$ decreases in a strictly monotonic fashion about a_0 (i.e., $S(a_0 + \xi) < S(a_0 - \xi)$ for all $\xi > 0$) then the orientation of the hysteresis loop in the first quadrant of the (x, r) plane is clockwise (since $A > 0$) whereas the loop in the third quadrant is counter-clockwise. If, on the other hand, the secant stiffness increases monotonically, the orientation is counter-clockwise in the first quadrant but clockwise in the third quadrant. See Fig. 4.

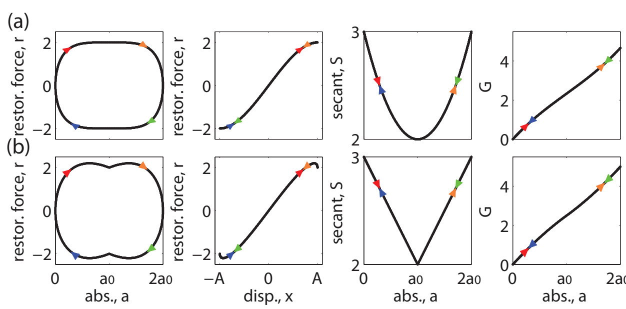

Fig. 3 Two element models (see Table 12) illustrate two situations where there is no hysteresis loop; $x(t) = A\sin(\omega t)$ with $A = 1$ and $\omega = 1$.

Property 3 (Smoothness of r, S, x and a)
The smoothness (i.e., differentiability classification) of $r(t)$ depends on the smoothness of both $x(t)$ and $S(a(t))$. If $S(a)$ and $x(t)$ are analytic functions, then:

$$\frac{dr}{dt} = \frac{d}{dt}(S(a)x) = S(a)\dot{x} + \frac{dS(a)}{da}x^2, \tag{21}$$

where $\dot{a} = x$ was used. However if $S(a)$ or $x(t)$ are non-differentiable at any point(s) in time, then care must be taken when interpreting Eq. (21). For example, the sharp outer tips

$$\text{Phase 1: } r = S(a_0 - \bar{a})\,x \quad \text{Red Arrow in Plots, with } 0 < t < \frac{T}{4}, \quad 0 < x(t) < A,\; 0 < a(t) < a_0, \quad a_0 > \bar{a}(t) > 0 \tag{17}$$

$$\text{Phase 2: } r = S(a_0 + \bar{a})\,x \quad \text{Orange Arrow in Plots, with } \frac{T}{4} < t < \frac{T}{2}, \quad A > x(t) > 0,\; a_0 < a(t) < 2a_0, \quad 0 < \bar{a}(t) < a_0 \tag{18}$$

$$\text{Phase 3: } r = S(a_0 + \bar{a})\,x \quad \text{Green Arrow in Plots, with } \frac{T}{2} < t < \frac{3T}{4}, \quad 0 > x(t) > -A,\; 2a_0 > a(t) > a_0, \quad a_0 > \bar{a}(t) > 0 \tag{19}$$

$$\text{Phase 4: } r = S(a_0 - \bar{a})\,x \quad \text{Blue Arrow in Plots, with } \frac{3T}{4} < t < T, \quad -A < x(t) < 0,\; a_0 > a(t) > 0, \quad 0 < \bar{a}(t) < a_0 \tag{20}$$

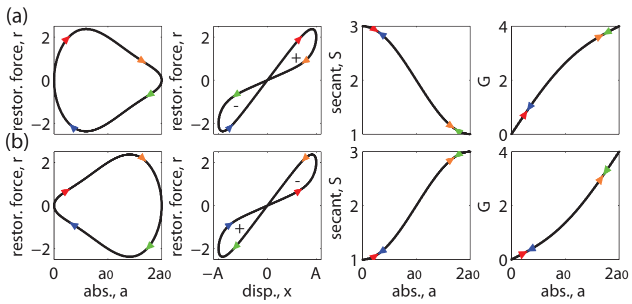

Fig. 4 Two element models (see Table 12) illustrate the relationship between the increasing/decreasing nature of $S(a)$ and the clockwise/counter-clockwise direction of (x, r); $x(t) = A\sin(\omega t)$ with $A = 1$ and $\omega = 1$.

of the "petals" (hysteresis loops) in Fig. 5 are due solely to the non-differentiability of the piecewise linear displacement in Eq. (13) at $t = \frac{T}{4}, \frac{3T}{4}$, whereas the outer tips are smooth in Fig. 4.

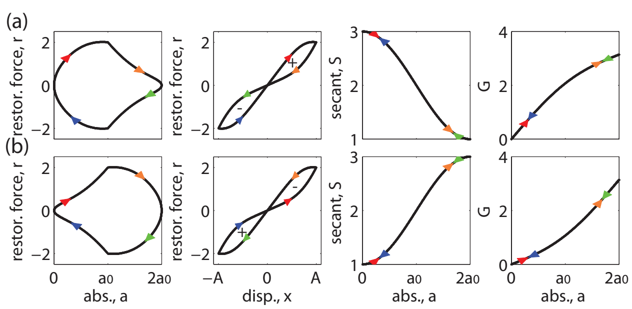

Fig. 5 The same element models as in Fig. 4 (see Table 12) but subject to $x(t) = \frac{4A}{T}\left(t - \frac{T}{2}\left\lfloor \frac{2t}{T} + \frac{1}{2}\right\rfloor\right)(-1)^{\lfloor \frac{2t}{T} + \frac{1}{2}\rfloor}$, with $a(0) = 0$, $T = \frac{2\pi}{\omega}$, $A = 1$, and $\omega = 1$.

Property 4 (Tangent Stiffness K along (x, r) Curve)

The tangent stiffness $K(t) = \frac{dr}{dx}(t)$ along the (x, r) path is symbolically obtained by dividing Eq. (21) by $\dot{x}(t)$ with the proviso that the velocity is not zero (although it is at $t = \frac{T}{4}, \frac{3T}{4}$):

$$K(t) = \frac{dr}{dx} = \frac{d}{dx}\left(S(a)x\right) = S(a) + \underbrace{\frac{dS(a)}{da}}_{\text{Factor 1}}\underbrace{\frac{x^2}{\dot{x}}}_{\text{Factor 2}} \tag{22}$$

Equation (22) shows that the tangent stiffness K and the secant stiffness S differ by a term that is critically sensitive (analytically and numerically) in the vicinity of times when $\dot{x} = 0$. This sensitivity is one of the reasons it is important to examine both S and K when analyzing test data with mem-models in mind (see Section 4.6). Moreover, if hysteresis is to be modeled well, it is important to study S and K separately from x and $\dot{x}$ in order to understand their effects on the restoring force r.

To clarify the relationship between secant and tangent stiffness, Table 5 gives the values of S and K for a few examples at $t = 0, \frac{T}{4}, \frac{T}{2}, \frac{3T}{4}, T$. These are the times when the (x, r) path either crosses the origin (when $x(t) = 0$), or the path reaches an extremum of $x(t)$ (when $\dot{x}(t) = 0$, $a(t) = a_0$), sometimes called a "turning point" in hysteresis modeling articles.

At the origin: For mem-springs of the form $r = S(a)x$, Eqs. (12) and (16) are continuous and equal to zero when $x(t) = 0$ while $\frac{dS}{da}$ is finite at those times, so one-sided limits exist and are continuous, leading to:

$$K(0) = S(a(0)) = S(0) \tag{23}$$

$$K\left(\frac{T}{2}\right) = S\left(a\left(\frac{T}{2}\right)\right) = S(2a_0) \tag{24}$$

$$K(T) = S(a(T)) = S(0) \tag{25}$$

for all examples in Figures 3-8.

At both turning points: Three situations are illustrated in Figs. 6 to 8, respectively. The situations are: (1) S is continuously differentiable with $\frac{dS}{da} = 0$; (2) S is continuous piecewise linear with $\frac{dS}{da} \neq 0$; (3) S has an integrable discontinuity with $\frac{dS}{da} = 0$. One-sided limiting values of S and K are given in Table 5 at each junction of Phases 1-4.

Under Situation (1) with the sinusoidal excitation – Fig. 6(a) – the product of Factors 1 and 2 in Eq. (22) may be determined by using L'Hospital's rule. Under Situation (1) with the piecewise excitation – Fig. 6(b) – Factor 1 is continuously differentiable and equal to zero while Factor 2 is zero – so their product is zero. Thus, the tangent stiffness is continuous and equal to the secant stiffness.

Under Situation (2) with the sinusoidal excitation – Fig. 7(a) – the tangential stiffness line becomes vertical. If the hysteresis loop in the first quadrant is considered a

Table 5 Values and S, K and U at the critical points within a cycle for selected models given in Section 3.3.

Fig. ID S, K or U	**Phase 1: Loading in 1st Quad.** $t = 0^+$	$t = \frac{T}{4}^-$	**Phase 2: Unloading in 1st Quad.** $t = \frac{T}{4}^+$	$t = \frac{T}{2}^-$	**Phase 3: Loading in 3rd Quad.** $t = \frac{T}{2}^+$	$t = \frac{3T}{4}^-$	**Phase 4: Unloading in 3rd Quad.** $t = \frac{3T}{4}^+$	$t = T^-$
4(a), 5(a), & 6(a)(b) S	3	2	2	1	1	2	2	3
7(a) S	3	1	1	1	1	1	1	3
7(b) S	3	1.33	1.33	1	1	1.33	1.33	3
8(a) S	3	2	1	0	0	1	2	3
11(a) S	3	3	1	1	1	1	3	3
4(a), & 7(a) K	3	$-\infty$	$+\infty$	1	1	$+\infty$	$-\infty$	3
5(a) K	3	-0.35	4.36	1	1	4.36	-0.35	3
6(a) K	3	-0.47	4.47	1	1	4.47	-0.47	3
6(b) K	3	2	2	1	1	2	2	3
7(b) K	3	-1.17	1.83	1	1	1.83	-1.17	3
8(a) K	3	-0.47	3.47	0	0	3.47	-0.47	3
11(a) K	3	3	1	1	1	1	3	3
4(a) U	$U(0) = 0$	$U\left(\frac{T}{4}\right) = 1.40$		$U\left(\frac{T}{2}\right) = 0.81$		$U\left(\frac{3T}{4}\right) = 1.40$		$U(T) = 0$
5(a) U	$U(0) = 0$	$U\left(\frac{T}{4}\right) = 1.29$		$U\left(\frac{T}{2}\right) = 0.58$		$U\left(\frac{3T}{4}\right) = 1.29$		$U(T) = 0$
6(a) U	$U(0) = 0$	$U\left(\frac{T}{4}\right) = 1.27$		$U\left(\frac{T}{2}\right) = 0.54$		$U\left(\frac{3T}{4}\right) = 1.27$		$U(T) = 0$
6(b) U	$U(0) = 0$	$U\left(\frac{T}{4}\right) = 1.16$		$U\left(\frac{T}{2}\right) = 0.31$		$U\left(\frac{3T}{4}\right) = 1.16$		$U(T) = 0$
7(a) U	$U(0) = 0$	$U\left(\frac{T}{4}\right) = 1.22$		$U\left(\frac{T}{2}\right) = 0.67$		$U\left(\frac{3T}{4}\right) = 1.22$		$U(T) = 0$
7(b) U	$U(0) = 0$	$U\left(\frac{T}{4}\right) = 1.04$		$U\left(\frac{T}{2}\right) = 0.45$		$U\left(\frac{3T}{4}\right) = 1.04$		$U(T) = 0$
8(a) U	$U(0) = 0$	$U\left(\frac{T}{4}\right) = 1.27$		$U\left(\frac{T}{2}\right) = 1.04$		$U\left(\frac{3T}{4}\right) = 1.27$		$U(T) = 0$
11(a) U	$U(0) = 0$	$U\left(\frac{T}{4}\right) = 1.5$		$U\left(\frac{T}{2}\right) = 1$		$U\left(\frac{3T}{4}\right) = 1.5$		$U(T) = 0$

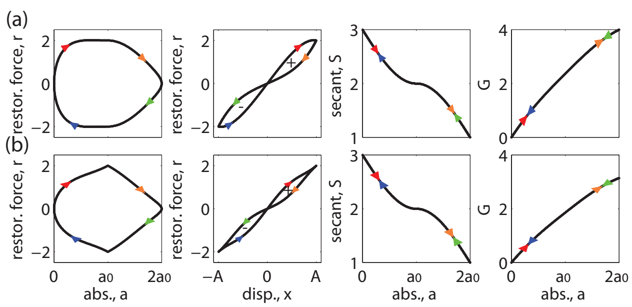

Fig. 6 The same element model (see Table 12) but subject to $x(t) = A\sin(\omega t)$, and $x(t) = \frac{4A}{T}\left(t - \frac{T}{2}\left\lfloor\frac{2t}{T} + \frac{1}{2}\right\rfloor\right)(-1)^{\lfloor\frac{2t}{T}+\frac{1}{2}\rfloor}$, with $a(0) = 0$, $T = \frac{2\pi}{\omega}$, respectively, with $A = 1$, and $\omega = 1$. This is to illustrate the impact of Situation (1) to the tangent stiffness of (x, r).

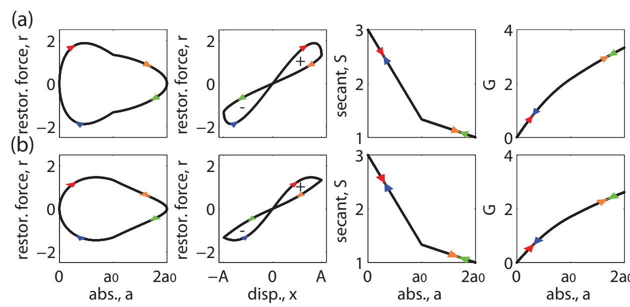

Fig. 7 The same element model (see Table 12) but subject to $x(t) = A\sin(\omega t)$, and $x(t) = \frac{4A}{T}\left(t - \frac{T}{2}\left\lfloor\frac{2t}{T} + \frac{1}{2}\right\rfloor\right)(-1)^{\lfloor\frac{2t}{T}+\frac{1}{2}\rfloor}$, with $a(0) = 0$, $T = \frac{2\pi}{\omega}$, respectively, with $A = 1$, and $\omega = 1$. This is to illustrate the impact of Situation (2) to the tangent stiffness of (x, r).

flower petal, its outer tip is rounded. This may be a disadvantage of this kind of excitation as it could mask discontinuities in the model in this situation. In Situation (2) with the the triangular excitation – 7(b) – $\dot{x}\left(\frac{T}{4}^-\right) \neq 0$, $\dot{x}\left(\frac{T}{4}^+\right) \neq 0$ and $\dot{x}\left(\frac{T}{4}^-\right) \neq \dot{x}\left(\frac{T}{4}^+\right)$. The last condition leads to $\frac{dr}{dx}\left(\frac{T}{4}^-\right) \neq \frac{dr}{dx}\left(\frac{T}{4}^+\right)$, under which we will always have a flower petal with a sharp outer tip.

Under Situation (3) – Fig. 8 – r has a $\mathcal{C}^0$ discontinuity at a_0, regardless of excitation.

Remark 11 (Rate Dependence of Mem-Spring Models)

Generally speaking, mem-spring models are rate dependent, behaving as linear (constant) springs "in the limit of infinite frequency" (Di Ventra et al (2009)). In particular, as $\omega \to \infty$ for models of the form $r = S(a)x$ subject to periodic input, we have $a_0 = \frac{A}{\omega} \to 0$, so $r(t) \to S(0)x(t)$ which is a linear spring.

Property 5 (Energy Stored or Dissipated)

For all examples in Figures 3 to 8, Table 5 gives the values of the energy $U(t)$ at the end of Phases 1-4. The results are in accord with passivity at the end of a full period, meaning $U(T) = U(0)$ as noted in Di Ventra et al (2009). In particular for $r = S(a)x$ subject to periodic input, energy is stored (created) during the first half period and then dissipated by an equal amount during the second half period (or vice versa). Moreover, because mem-springs degenerate to linear springs as the frequency goes to infinity (Remark 11), $U(t)$ goes to zero in the same limit.

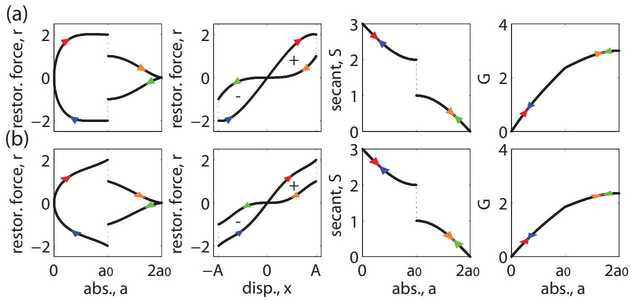

Fig. 8 The same element model (see Table 12) but subject to $x(t) = A\sin(\omega t)$, and $x(t) = \frac{4A}{T}\left(t - \frac{T}{2}\left\lfloor \frac{2t}{T} + \frac{1}{2}\right\rfloor\right)(-1)^{\lfloor \frac{2t}{T}+\frac{1}{2}\rfloor}$, with $a(0) = 0$, $T = \frac{2\pi}{\omega}$, respectively, with $A = 1$, and $\omega = 1$. This is to illustrate the impact of Situation (3) to the tangent stiffness of (x, r).

3.4 The Usefulness of System Models

According to Property 5, the simplest mem-spring models show energy storage in either the first or the third quadrant, whereas data from many structural (macro-scale) tests show only energy dissipation (in both quadrants); e.g., see Dolce et al (2000); Santos and Cismaşiu (2007); Christopoulos et al (2008); Ricles et al (2002)) and Fig. 9 for one such example. A different insight can be gained by contrasting Eqs. (17) and (19) while observing that an element model cannot produce the same behavior in the first and third quadrants when subjected to the specified cyclic input. In other words, the (x, r) path is "anti-symmetric with respect to the origin", as stated in Di Ventra et al (2009).

One way to tackle this issue within the framework of mem-models is to utilize system models, Table 2, Line 5. The basic approach is to include x in S and introduce a switching mechanism whenever $x(t) = 0$. Section 5 presents examples of such mem-spring system models. The rest of this subsection gives a few examples of mem-springs of the form $r = S(a, x)x$ subject to the same two types of periodic input as were used in the previous subsection (Table 4). Table 13 in Appendix B contains the secant stiffness $S(a, x)$ and Table 6 lists values of S, K and U (for comparison with Table 5). Contrasting Fig. 10 with 4, and Fig. 11(a) with (b), one can see the difference that the switching in these models can make in terms of modeling capability. Properties 1 to 4 may be extended from elements to systems; see Figs. 26 and 27 in Appendix B for an example.

4 CASE STUDIES OF MEM-DASHPOTS

4.1 Overview of Mem-Dashpot Case Studies

As a case study of a mem-dashpot in the engineering mechanics literature, details of a controllable hydraulic damper in Scruggs and Gavin (2010) are presented and discussed in this section. For comparison purposes, results from three

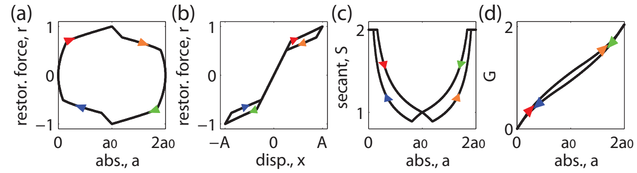

Fig. 9 (b) Following Fig. 1 in Santos and Cismaşiu (2007), a schematic hysteretic loop is formed for SMA subject to $x(t) = \frac{4A}{T}\left(t - \frac{T}{2}\left\lfloor \frac{2t}{T} + \frac{1}{2}\right\rfloor\right)(-1)^{\lfloor \frac{2t}{T}+\frac{1}{2}\rfloor}$, with $a(0) = 0$, $T = \frac{2\pi}{\omega}$, $A = 1$, and $\omega = 1$. (a), (c), and (d) Other insights developed in this study. See Appendix D including Fig. 30 for more explanations.

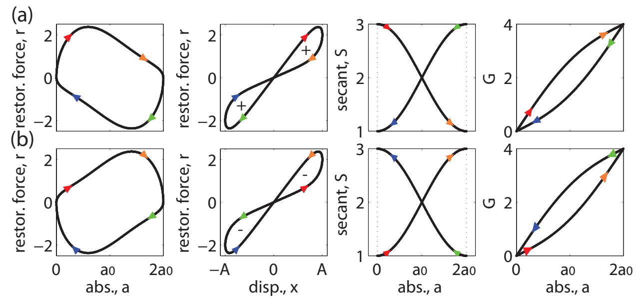

Fig. 10 Two system models (see Table 13) that contrast the two element models in Fig. 4 and illustrate the behavior of (x, r) in the third quadrant; $x(t) = A\sin(\omega t)$ with $A = 1$ and $\omega = 1$.

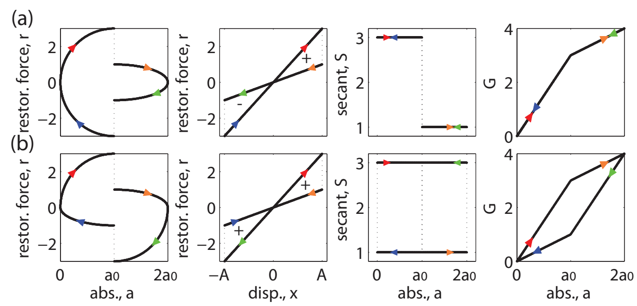

Fig. 11 One element contrasted with one system model (see Table 13) to illustrate the behavior of (x, r) in the third quadrant; $x(t) = A\sin(\omega t)$ with $A = 1$ and $\omega = 1$.

nano-device models (two memristors and one memristive system in Strukov et al (2008); Strukov (2011); Chang et al (2011)) are also summarized and discussed. The three nano-device models, designated herein as Case Studies #1, 2 and 3 (see Appendix C.1), can be viewed as mem-dashpots by means of the Force-Voltage Analogy. Instead of using the Simulation Program with Integrated Circuit Emphasis (SPICE) as in Chang et al (2011), MATLAB was used for all computations herein. Throughout this study, ode45 (a MATLAB ODE solver based on RK45) was used with RelTol = 10^{-6}, AbsTol = 10^{-3} and MaxStep = 10^{-3}.

This section focuses on the governing state and input-output equations. Naturally the input (i.e., excitation) plays an important role in understanding the nonlinear input-output equations. Although the response to many different kinds of excitation are of interest, only a few signal

Table 6 Values and S, K and U at the critical points within a cycle for selected models given in Section 3.4.

Fig. ID S, K or U	Phase 1: Loading in 1st Quad. $t=0^+$	$t=\frac{T}{4}^-$	Phase 2: Unloading in 1st Quad. $t=\frac{T}{4}^+$	$t=\frac{T}{2}^-$	Phase 3: Loading in 3rd Quad. $t=\frac{T}{2}^+$	$t=\frac{3T}{4}^-$	Phase 4: Unloading in 3rd Quad. $t=\frac{3T}{4}^+$	$t=T^-$
10(a) S	3	2	2	1	3	2	2	1
11(b) S	3	3	1	1	3	3	1	1
26(a) (b) & 27(a) (b) S	3	1	1	3	3	1	1	3
10(a) K	3	$-\infty$	$+\infty$	2	3	$-\infty$	$+\infty$	1
11(b) K	3	3	1	2	3	3	1	1
26(a) K	3	$-\infty$	1	3	3	$-\infty$	1	3
26(b) K	3	-3	1	3	3	-3	1	3
27(a) K	3	-5.00	1	3	3	-5.00	1	3
27(b) K	3	1	1	3	3	1	1	3
10(a) U	$U(0)=0$	$U\left(\frac{T}{4}\right)=1.40$		$U\left(\frac{T}{2}\right)=0.81$		$U\left(\frac{3T}{4}\right)=2.22$		$U(T)=1.62$
11(b) U	$U(0)=0$	$U\left(\frac{T}{4}\right)=1.5$		$U\left(\frac{T}{2}\right)=1$		$U\left(\frac{3T}{4}\right)=2.5$		$U(T)=2$
26(a) U	$U(0)=0$	$U\left(\frac{T}{4}\right)=1.33$		$U\left(\frac{T}{2}\right)=0.58$		$U\left(\frac{3T}{4}\right)=1.92$		$U(T)=1.17$
26(b) U	$U(0)=0$	$U\left(\frac{T}{4}\right)=1$		$U\left(\frac{T}{2}\right)=0.25$		$U\left(\frac{3T}{4}\right)=1.25$		$U(T)=0.5$
27(a) U	$U(0)=0$	$U\left(\frac{T}{4}\right)=1.12$		$U\left(\frac{T}{2}\right)=0.50$		$U\left(\frac{3T}{4}\right)=1.62$		$U(T)=1.01$
27(b) U	$U(0)=0$	$U\left(\frac{T}{4}\right)=0.79$		$U\left(\frac{T}{2}\right)=0.17$		$U\left(\frac{3T}{4}\right)=0.96$		$U(T)=0.34$

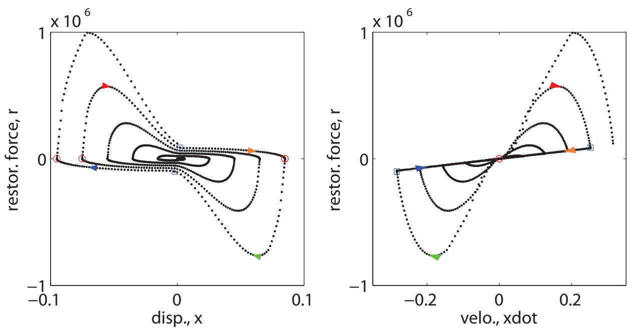

Fig. 12 These two panels reproduce Scruggs and Gavin (2010) but acceleration turning points (and others) have been added here.

types have actually been used thus far, namely periodic, ordered, or amplitude-modulated forms, which are often used to probe both memristive devices and engineering mechanics devices.

4.2 A Controllable Hydraulic Damper

Equations (30.59) to (30.62) in Scruggs and Gavin (2010) are simplified versions of a more general form of variable damper, also reviewed in that same paper. Following the notation for flow-controlled memristive systems in Tables 2 and 3, Eqs. (30.59) to (30.62) can be re-written as time-invariant state and input-output, Eqs. (26) and (27), where the state vector has two components $\mathbf{y}(t) = [y_1(t), y_2(t)] = [x(t), w(t)]$ with $w \in [0, 1]$. T_w, K_w, $c_{\min}$ and $c_{\max}$ are design parameters, while sat and $\mathcal{H}$ denote the saturation and Heaviside functions, respectively. Thus this model is included as a key mem-dashpot case study. Some snapshots of this non-trivial model from Scruggs and Gavin (2010) are reproduced in Fig. 12, while more details and insights are provided in Figs. 12 and 13.

4.3 Regarding Variable(s) in State Vector $\mathbf{y}$

The selection of variable(s) in state vector $\mathbf{y}$ is, in general, a subjective matter that depends on the physical mechanism(s) perceived to underlie the observed nonlinear behavior. In some cases encountered in the literature, a mem-model expressed in terms of a state vector does not necessarily mean the model is a system as defined in Table 2. Instead, the model may actually be an element (as in Case Study #1). Two interesting observations can be made regarding Case Study #2. First, it is straightforward to show that:

$$
\begin{aligned}
v(t) &= \left[y + \frac{R_{ON}}{R_{OFF}}(1-y)\right]\frac{D^2}{\mu_V}\frac{\dot{y}}{y(1-y)} \\
&= \underbrace{\frac{D^2}{\mu_V}\left[\frac{1}{1-y} + \frac{R_{OFF}}{R_{ON}}\frac{1}{y}\right]}_{D(y)}\dot{y}
\end{aligned}
\tag{28}
$$

where $y = \frac{w}{D}$, which may have a physical meaning of being a normalized width according to Chang et al (2011). It can be seen that y, $\dot{y}$ - joined with v - form a memristor (not a memristive system). We have:

$$
\begin{aligned}
G(y) &= \int g(y)dy \\
&= \frac{D^2}{\mu_V}\left[-\ln(1-y) + \frac{R_{OFF}}{R_{ON}}\ln y\right] \\
&\quad + \frac{D^2}{\mu_V}\left[\ln(1-y_0) - \frac{R_{OFF}}{R_{ON}}\ln y_0\right]
\end{aligned}
\tag{29}
$$

where $\ln y$ and $\ln(1-y)$ require $0 < y < 1$.

Alternatively, it is again straightforward to show that the state and input-output equations in Case Study #2 define another memristor. We can also show that:

$$
v = \left[\frac{R_{ON} - R_{OFF}}{e^{-\left(\mu_V \frac{R_{ON}}{D} q + C\right)} + 1} + R_{OFF}\right] i
\tag{30}
$$

$$\text{State Eq.:}\quad \dot{\mathbf{y}} = \underbrace{\begin{bmatrix} \dot{x} \\ \frac{1}{T_w}\,\text{sat}_{[-1,1]}\left\{K_w\left[50|y_1|^{\frac{3}{2}}\mathcal{H}\left(-\left[(1-y_2)\,c_{\min}+y_2c_{\max}\right]A_p^2\dot{x}\cdot y_1\right)-y_2\right]\right\}\end{bmatrix}}_{\mathbf{g}(\mathbf{y},\dot{x})} \tag{26}$$

$$\text{I/O Eq.:}\quad r = \underbrace{\left[(1-y_2)c_{\min}+y_2c_{\max}\right]A_p^2}_{D(\mathbf{y},\dot{x})}\,\dot{x} \tag{27}$$

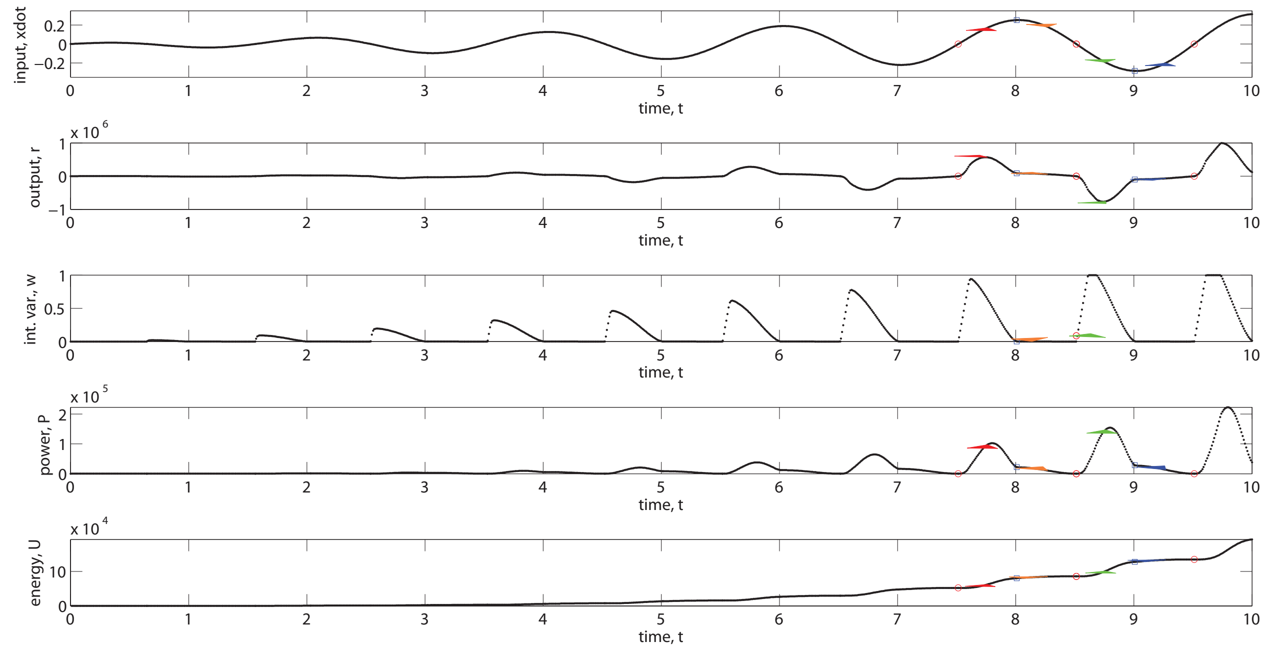

Fig. 13 Time histories of the input, output, internal variable, power and energy in Fig. 30.62 in Scruggs and Gavin (2010).

where C is an integral constant to be determined (i.e., a memristor, not a memristive system).

Considering what variable(s) a state vector might include, the internal state variable w in Scruggs and Gavin (2010) has a physical interpretation, being the normalized viscosity coefficient with $w \in [0, 1]$, which is quite noteworthy because in Case Study #3 from Chang et al (2011), a similar choice occurs for the internal state variable w. The normalized w has a clear physical interpretation, being an area index varying between 0 and 1. w can be solved as a nonlinear function involving an integral of v. Using the notation in Table 2, w is a nonlinear function of ϕ while W is an affine combination of w and a nonlinear function of v. Ultimately, W can be expressed as a nonlinear bivariate function of v and ϕ; see Appendix C.2.

4.4 Regarding Excitations

The first (and maybe foremost) challenge in studying mem-models is the dependence of their responses on their excitations, which is due to their intrinsic nonlinearity (so long as the amplitude of excitation is high enough to meet some nonlinearity observability criteria). See Figs. 17 to 19 (later) for simulated results of Case Studies #1 to 3 as well as the hydraulic damper from Scruggs and Gavin (2010). To symbolically illustrate excitation-dependency, let $r = D(x, \dot{x})\,\dot{x}$, which is a simple example of a flow-controlled time-invariant system model for a mem-dashpot, we have:

$$\begin{aligned} p &= \int r dt = \int D(x, \dot{x})\,\dot{x} dt \\ &= \int D(x, \dot{x})\,dx = \int D(x, h(x))\,dx \end{aligned} \tag{31}$$

where $\dot{x} = h(x)$ has a piecewise-defined expression according to the phase plot $(\dot{x}, x)$ - as discussed in Section 3.3 especially Table 4 and Eqs. (17) to (20) - but for a mem-dashpot. Thus, it can be seen that p is piecewise defined, depending on x. Also, it can be seen that (x, p) (or, equivalently, G in Table 2) is phase-plot-dependent, i.e., excitation-dependent.

Together with Fig. 2, Fig. 14 exemplifies typical time histories and phase plots in terms of x and $\dot{x}$ used as input to a flow-controlled mem-dashpot. Similar phase plots, but in terms of p and r, could be applied to an effort-controlled mem-dashpot. (For a mem-spring, we could use pairs of a

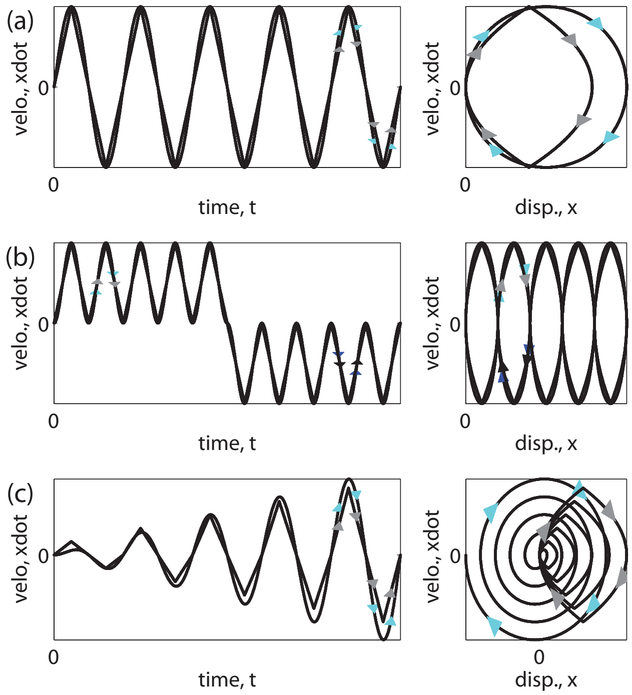

Fig. 14 Typical smooth and nonsmooth excitation time histories and their corresponding phase plots. Here, a mem-dashpot is used as an example. (a) follows Fig. 2; (b) mimics Chang et al (2011); the analytic signal in (c) follows Scruggs and Gavin (2010) while the piecewise signal in (c) mimics Ricles et al (2002).

and x and p and r, respectively, for a flow-controlled and an effort-controlled situation.)

Each of the three typical signals illustrated in Fig. 14 has its pros and cons. In terms of propagating in phase space, the sinusoidal signal seems to be the least efficient given that only one circle is explored (assuming constant amplitude). An amplitude-modulated signal would be more efficient in contrast in this regard.

The difference between a smooth signal and its sawtooth counterpart needs to be clarified: the former is differentiable, thus facilitating analytical manipulation, while the latter does not possess this convenience but enjoys popularity in practice, e.g., in pseudo-dynamic tests in earthquake engineering (such as the excitation in Fig. 20(a) following Applied Technology Council (2001)). Of course, these excitation forms are not exhaustive. Ultimately, responses under random excitations need to be studied; studying periodic and/or ordered excitations is a necessary preliminary stage.

4.5 Regarding Solving State and Input-Output Equations

State and input-output equations, such as Eqs. (5) and (6) and others presented elsewhere as typical examples of flow/effort-controlled mem-dashpot and mem-spring systems, can be sometimes be solved uncoupled. For example, Case Studies #1 to 3 are simple enough that they can be solved uncoupled (as they were in this work; see Section 4.3 and Appendix C.1). On the other hand, the hydraulic damper equations from Scruggs and Gavin (2010) were solved coupled.

In particular, Eq. (5) is a nonlinear ODE to be solved. The smoothness condition for numerically integrating this ODE can easily be violated by discontinuities in the nonlinear operator $\mathbf{g}$ and/or those in the input $\dot{x}$. The former leads to state events while the latter to time events. See Fig. 14, where a sawtooth wave is an example involving time events; typically a displacement time history with sawtooth features is popular in earthquake engineering tests. Mathematically, this means that $\frac{dx}{dt}$ is discontinuous at certain times. On the other hand, non-smooth operators $\mathbf{f}$ include, but are not limited to, piecewise-defined functions or generalized functions. Time events, which are (by definition) known prior to the start of computations, are associated with excitations (assuming they are deterministic, not random). Some locations when $\dot{x} = 0$ (or $i = 0$, or $v = 0$) are highlighted with red circles in most plots in Section 4. In contrast, state events cannot be known in advance because they are caused by nonlinearities in the constitutive relations. Both directly affect the smoothness of the state equation, an ODE.

An interesting and a challenging point for the controllable hydraulic damper is the subtlety of state events. There are no time events in this case because the prescribed excitation is analytic. However there are state events, caused by four situations, detailed in Table 7. Numerically solving the case study of controllable hydraulic damper can be quite challenging. We need to pay attention to the time instances when $x(t) = 0$, $\dot{x}(t) = 0$, $\ddot{x}(t) = 0$ and those time instances when sat applies. One of the challenges - for the specified excitation time histories - is that $x(t) = 0$ and $\ddot{x}(t) = 0$ do not line up. Some locations when $\ddot{x} = 0$ (or $\dot{v} = 0$) are highlighted with blue squares in most plots in Section 4.

4.6 Using Time-Varying Secants in Modeling

For modeling purposes, it is worth noticing that the quotient of $r(t)$ and $\dot{x}(t)$ has the physical meaning of a time-varying viscous damping coefficient. Likewise the quotient of $r(t)$ and $x(t)$ is a time-varying stiffness. In other words, the quotients $D = \frac{r(t)}{\dot{x}(t)}$ and $S = \frac{r(t)}{x(t)}$ are time-varying secants, illustrated in Fig. 15, which are defined for all t except when the denominator is zero which should not hinder physical interpretation.

Given a time-varying (x, r) plot, the physical interpretation of secant stiffness S clearly differs from the tangent stiffness K, as discussed in Property 4 and shown in Tables 5 and 6. Secant modulus is also well-known in engineering mechanics as, for example, Young's modulus for concrete which is typically estimated for a stress-strain curve by con-

Table 7 State events in Case Study of controllable hydraulic damper.

ID	Description
(i)	those caused by $\mathcal{H}$, i.e., both $x(t) = 0$ and $\dot{x}(t) = 0$
(ii)	those caused by sat, which are not known in advance. When the excitation is low, however, we do not need to worry about this type of state event
(iii)	those caused by the absolute value function, i.e., $x(t) = 0$
(iv)	those caused by the "hard bound" of w, i.e., $w \in [0, 1]$ - It is found that, for the specified parameter values, this bound is easier to reach than the bound by sat.

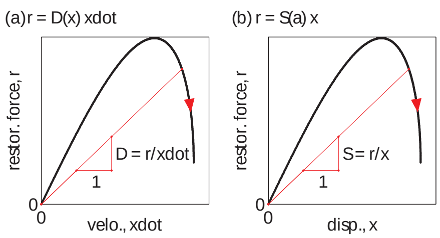

Fig. 15 Cartoons showing time-varying secants of (a) ($\dot{x}$, r) and (b) (x, r) for memristive and memcapacitive systems, respectively.

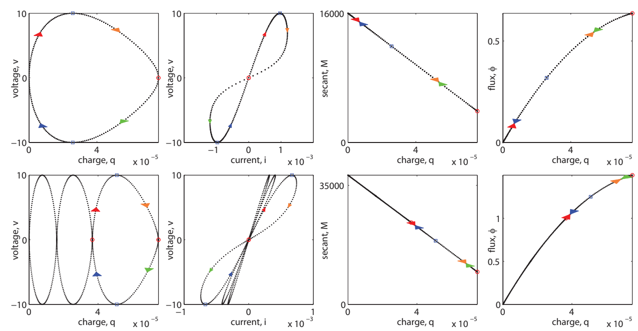

Fig. 17 Fig. 2b and 2c in Case Study #1 from Strukov et al (2008) are reproduced by using the two different memristor models subject to two different excitations. See Tables 14 and 15 in Appendix C.1 for details.

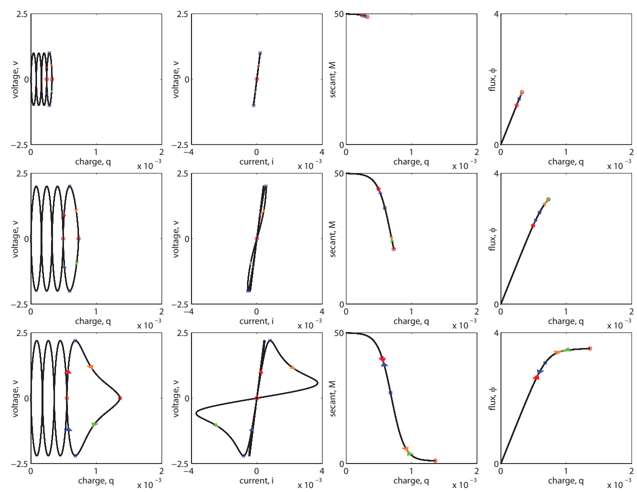

Fig. 18 A parametric study based on the model given in Strukov (2011), Page 17, subject to $v = \pm v_0 \sin^2\left(\frac{1}{2} 2.5\pi t\right)$ with v_0 = 1, 2, 2.2, respectively. These exercises reveal the one-to-one mapping M (or, equivalently, G) as the excitation gets stronger. They also show that a memristor may not display its nonlinearity when the excitation is very weak. This is our Case Study #2; see Tables 14 and 15 in Appendix C.1 for details.

necting the origin with the point corresponding to 45% of its ultimate strength in accord with the recommendation of ACI (ACI Committee 318 (2011)). However, time-varying secants are not so widely used as time-varying tangents when modeling path-dependent engineering mechanics systems. Nevertheless, when applying mem-models to experimental data, we must pay attention to time-varying secants . For the reader's convenience, time-varying secant plots of all four mem-dashpots are presented together in Fig. 16. Note that Cases #1 to 3 are effort-controlled with $v(t)$ specified as the excitation; $M = \frac{v(t)}{i(t)}$ and $W = \frac{i(t)}{v(t)}$ in these case studies are analogous to $\frac{r(t)}{\dot{x}(t)}$ and $\frac{\dot{x}(t)}{r(t)}$, respectively, for mem-dashpots.

Example 1 (Using $M = \frac{v(t)}{i(t)}$ for Modeling Memristors: Case Studies #1 and 2)

Figures 17 and 18 show results from Case Studies #1 and 2. Even though different excitations are used, each quotient $M = \frac{v(t)}{i(t)}$ stays on its own secant curve, which is a constitutive curve. Moreover, since these are memristors (elements), each flux-charge relationship is one-to-one for the specified excitation, which in general does not happen for systems (either memristive or memcapacitive).

Example 2 (Using $W = \frac{i(t)}{v(t)}$ for Modeling a Memristive System: Case Study #3)

Figure 19 shows results from Case Study #3 (Chang et al (2011)), which is a memristive system (not an element). For this model, the secant (i.e., quotient) is a bivariate function which depends on the voltage v and its time integral ϕ. In addition, both (q, ϕ) and (W, ϕ) are not one-to-one mappings - even though these facts are not obvious without careful study of the model and Fig. 19. While Appendix C.2 discusses these claims, intuitively we explain them as a result of the model not being an element but a system, the former of which would guarantee (q, ϕ) and (W, ϕ) to be one-to-one mappings according to Table 8.

Example 3 (Using $D = \frac{r(t)}{\dot{x}(t)}$ for Modeling a Mem-Dashpot: Scruggs and Gavin (2010))

It should not be a surprise to learn that, for memristive systems, the secant damping D is not a single-valued function of x. For example, under the excitation given

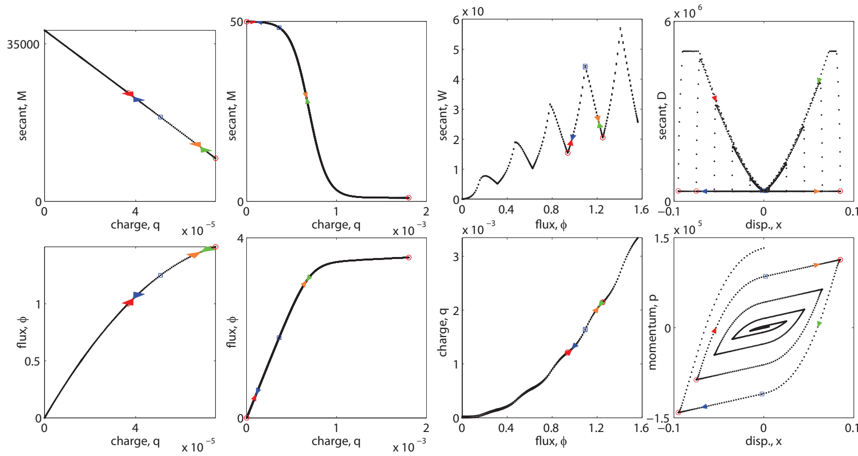

Fig. 16 Top Row: The secants for all four case studies; the complexity increases from elements (first two plots) to systems (last two plots). For an element, the secant is a one-to-one mapping. For a system, it is not. For Case Study #3, the secant is a bivariate function (see Fig. 19). For the controllable hydraulic damper, it is a dynamic quantity. Bottom Row: The integrals of the secants.

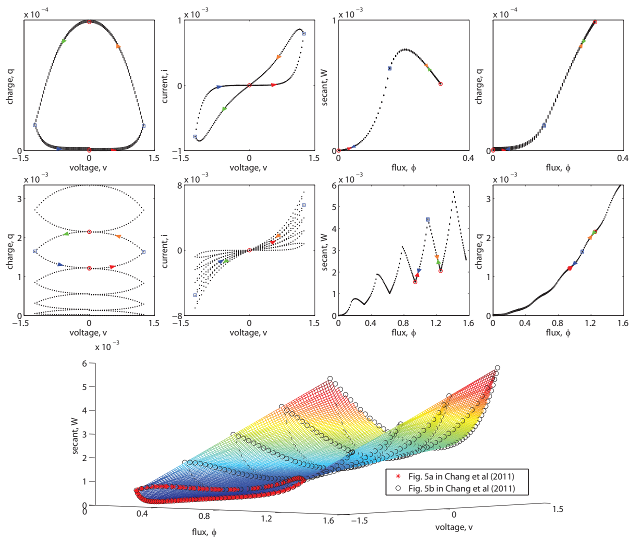

Fig. 19 An illustration of the secant W being a bivariate function of ϕ and v in Case Study #3 from Chang et al (2011). The three-dimensional surface $W = W(\phi, v)$ contains two trajectories that resulted from two distinct excitations. In addition, the first and third quadrants in (v, i) correspond to two different curves in (W, ϕ) and (q, ϕ), even though these facts may not be easily seen here. See Appendix C.2.

in Scruggs and Gavin (2010), the secant damping in $(\dot{x}, r)$ is not a simple function. In fact, the internal state variable, w, is actually a normalized time-varying damping coefficient that follows its own dynamics; see Fig. 13.

5 CASE STUDIES OF MEM-SPRINGS

5.1 Overview of Mem-Spring Case Studies

In this section, we present mem-spring models that reproduce the features of some fascinating nonlinear hysteresis which we believe have underlying memcapative nature. In contrast to memristors, memcapacitors are relatively new, yet we believe there is no lack of examples. Two possibilities are self-centering structures and flag-shaped hysteresis, which have captured attention in earthquake engineering and shape memory alloy (SMA) communities (e.g., Ricles et al (2002); Christopoulos et al (2008)). However they are neither memristors nor memristive systems. The zero-crossing property of memristors is expressed in terms of $(\dot{x}, r)$, whereas the zero-crossing property of self-centering structures (or flag-shaped hysteresis) is expressed in terms of (x, r) manifesting super-elasticity, i.e., having zero residual displacement upon unloading. Perhaps their behavior could be modeled as memcapacitors or, more likely, memcapacitive systems. While simulated data is used for SMA as described Appendix D, experimental data is examined for a self-centering test structure in this subsection. In both cases, the resulting mem-spring models utilized the switching mechanism discussed in Section 3.4.

There are of course other mechanical capacitors (i.e., springs) that include memory effects; however many of them are neither memcapacitors nor memcapacitive systems. For example, the Ramberg-Osgood model (Jennings (1964)) is not a memcapacitor, nor is it a memcapacitive system. The same can be said for the well-known bilinear model (Caughey (1960b,a); Kalmár-Nagy and Shekhawat (2009)).

5.2 Experimental PC4 Data Modelled as a Mem-Spring

PC4 in Ricles et al (2002) is a specimen typifying the potential of self-centering structures. $T = 8$ seconds is assumed for every cycle of an amplitude modulated sawtooth displacement excitation as shown in Fig. 20(a). Four colors are used to indicate loading and unloading in both the positive and negative directions. Digitized data is only obtained for the positive direction while antisymmetry is used for the

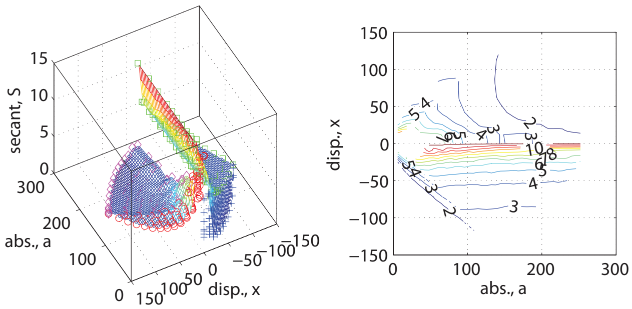

Fig. 22 The function $S = S(a, x)$ was fit piecewisely with nonsmooth surfaces using the digitized data.

negative direction. $a(t)$ is obtained through calculating the area under $x(t)$. Fig. 21(a) recovers Ricles et al (2002)'s Fig. 8(a), while Fig. 20(b) to (d) and Fig. 21(b) and (c) provide other quantities that are not presented in Ricles et al (2002) but useful in our modeling.

For the assumed excitation, the secant stiffness S shown in Fig. 22 was extracted by analyzing test data. To clarify this, we select a and $\dot{x}$ as state variables and assume the following input-output equation:

$$r = S(\underbrace{a, \dot{x}}_{\mathbf{y}}, x)x \tag{32}$$

$$\begin{aligned} &= \left[\frac{1}{4}(\text{sgn}(x) + 1)(\text{sgn}(\dot{x}) + 1)S_1(x) \right. \\ &+ \frac{1}{4}(\text{sgn}(x) + 1)(1 - \text{sgn}(\dot{x}))S_2(a, x) \\ &+ \frac{1}{4}(1 - \text{sgn}(x))(1 - \text{sgn}(\dot{x}))S_3(x) \\ &\left. + \frac{1}{4}(1 - \text{sgn}(x))(\text{sgn}(\dot{x}) + 1)S_4(a, x) \right] x \end{aligned} \tag{33}$$

For this example, having $\dot{x}$ as a state variable is very helpful in defining the switching mechanism for a memcapactive system. For each of the four zones selected by the joint signs of x and $\dot{x}$, the value of S is either a function of x alone (when it seems to be simply a nonlinear spring) or a function of both a and x (when it seems to be a memcapacitive system).

Our proposed model works with the specified amplitude and rate of the input. It is a black-box model that is quite a simplification since it involves only a single-degree-of-freedom. Since each nonlinear model would be different, our model must be checked against additional test data. In addition, we anticipate the need for a damage index bounded within a range, to be introduced as an internal state variable.

5.3 A Proposed Qualitative Mem-Spring Model for Flag-Shaped Hysteresis

When an input $x(t)$ with a period of $T = 4$ seconds is used, we have the following model and simulation shown in Figs. 23 and 24 by introducing an intermediate variable, which is <u>not</u> a state variable:

$$\begin{aligned} &w(t) = a(t) - a(t_i)\left[\mathcal{H}(t - t_i) - \mathcal{H}(t - t_{i+1})\right] \\ &\quad t \in [t_i, t_{i+1}], \;\; \text{where } x(t_i) = 0, \;\; i = 1, 2, 3, \ldots \end{aligned} \tag{34}$$

leading to $w(t) = a(t)$ when $x(t) > 0$, and $w(t) = a(t)-$ a local maximum value for $a(t)$ when $x(t) < 0$. All local maximum values can be considered values of a memory parameter (Wright and Pei (2012)). The input-output equation then becomes the following:

$$S(t) = \begin{cases} S_0 e^{-a_0}, & |w(t)| < a_0 \\ S_0 e^{-|w(t)|}, & |w(t)| > a_0 \end{cases} \tag{35}$$

where $a_0 > 0$. Comparing Figs. 20 with 23, and 21 with 24 indicate both the promise and limitation of this proposed mem-spring model in capturing the flag-shaped hysteresis given in the PC4 data in Ricles et al (2002).

5.4 Comment on Generalizing Mem-Springs

Many continuum mechanics texts introduce constitutive models by discussing linearly elastic materials that obey tensorial stress-strain equations

$$\boldsymbol{\sigma} = \mathbf{E} : \boldsymbol{\varepsilon} \tag{36}$$

where $\mathbf{E}$ denotes a constant tensor called the secant modulus (Willam (2002)). These are called Hookean models because they generalize Hooke's law, which is a scalar equation, just as each input-output equation in Table 2 is scalar. By analogy, one way to generalize mem-springs is to embed them in continuum mechanics by defining a secant modulus tensor which depends on strain as well as other state variables $\mathbf{y}$ that enable history dependence $\mathbf{E} = \mathbf{E}(\mathbf{y}, \boldsymbol{\varepsilon})$.

For example, consider a long thin uniform cylindrical wire, made of SMA, having length L and cross-sectional area A. Assume infinitesimal strain theory, let the axial displacement be denoted by

$$\delta = \delta(\xi, t) \tag{37}$$

where $\xi \in [0, L]$ is the axial coordinate, and let

$$\varepsilon = \varepsilon(\xi, t) = \frac{\partial \delta(\xi, t)}{\partial \xi} \tag{38}$$

be the axial strain. Assume the SMA material obeys a uniaxial stress-strain equation of the form

$$\sigma = E(\alpha, \varepsilon)\varepsilon \tag{39}$$

where $\alpha = \alpha(\xi, t)$ is the integral of the strain with respect to time, called the "strain absement", thereby enabling

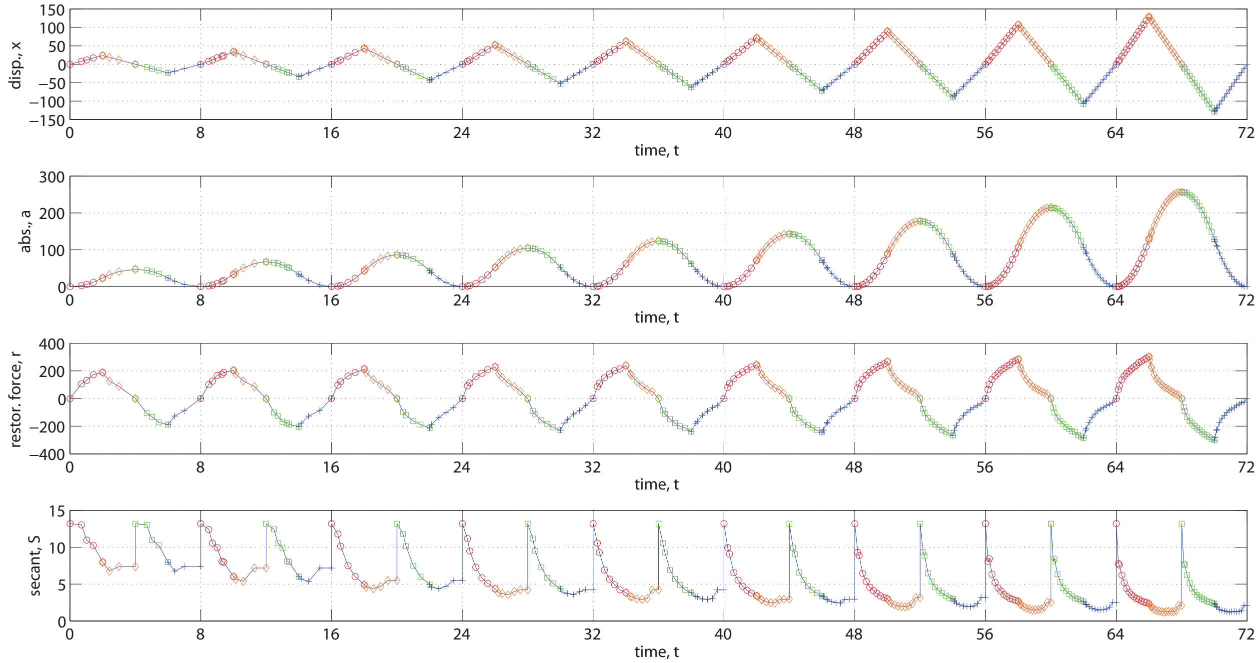

Fig. 20 All time histories reconstructed to study Specimen "PC4" in Ricles et al (2002)'s Fig. 8(a).

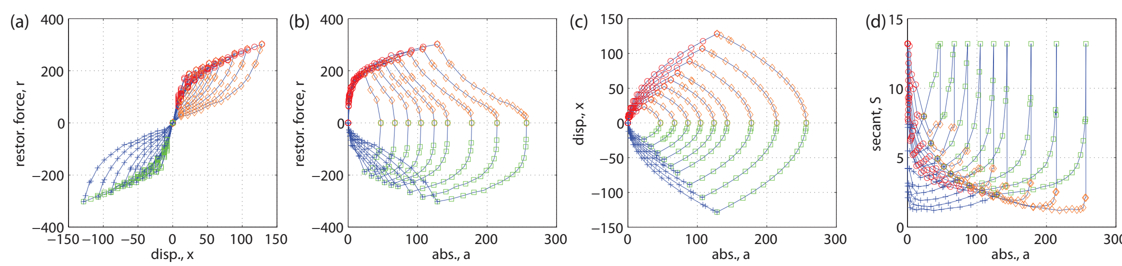

Fig. 21 (x, r), (a, r), (a, x) and (a, S) are shown here, where (a) matches Ricles et al (2002)'s Fig. 8(a), and (b) to (d) are derived from (a) and to reveal the insights for modeling in this study.

history-dependent response under certain axial loading conditions. Furthermore, since SMA is known to be rate dependent (Zhu and Zhang (2007)), the secant modulus should also depend on strain rate $\varepsilon_t = \frac{\partial \varepsilon(\xi,t)}{\partial t}$, so generalize further by letting

$$E = E(\alpha, \varepsilon_t, \varepsilon) \tag{40}$$

which highlights the distinction between history- and rate-dependent response. The local axial stiffness of this model is

$$S(\alpha, \varepsilon_t, \varepsilon) = \frac{E(\alpha, \varepsilon_t, \varepsilon)A}{L} \tag{41}$$

which is analogous to the secant stiffness in Eq. (32). Dynamically, this SMA wire model would satisfy the nonlinear wave equation

$$\mu \frac{\partial^2 \delta}{\partial t^2} = \frac{\partial}{\partial \xi}\left[E(\alpha, \varepsilon_t, \varepsilon)\frac{\partial \delta}{\partial \xi}\right] \tag{42}$$

where μ is the mass density of the SMA material.

In addition to nonlinear material behavior, nonlinear geometric behavior (finite strain) must ultimately be considered in three-dimensional configurations. As stated on page 609 of Willam (2002), "the three versions of nonlinear elasticity" (algebraic, integral, differential) "lead to constitutive formulations which exhibit fundamental differences when we consider triaxial conditions." Constitutive models for SMA (and other materials) must be generalized beyond nonlinear elasticity, thereby enabling hysteretic dissipative response under diverse loading conditions. These are challenging topics which have been, and will continue to be, important areas of engineering mechanics research for many decades.

6 SUMMARY AND CONCLUSIONS

In brief, Chua proposed the memristor in Chua (1971), presented memristive systems theory with Kang five years later in Chua and Kang (1976), and presented memcapac-

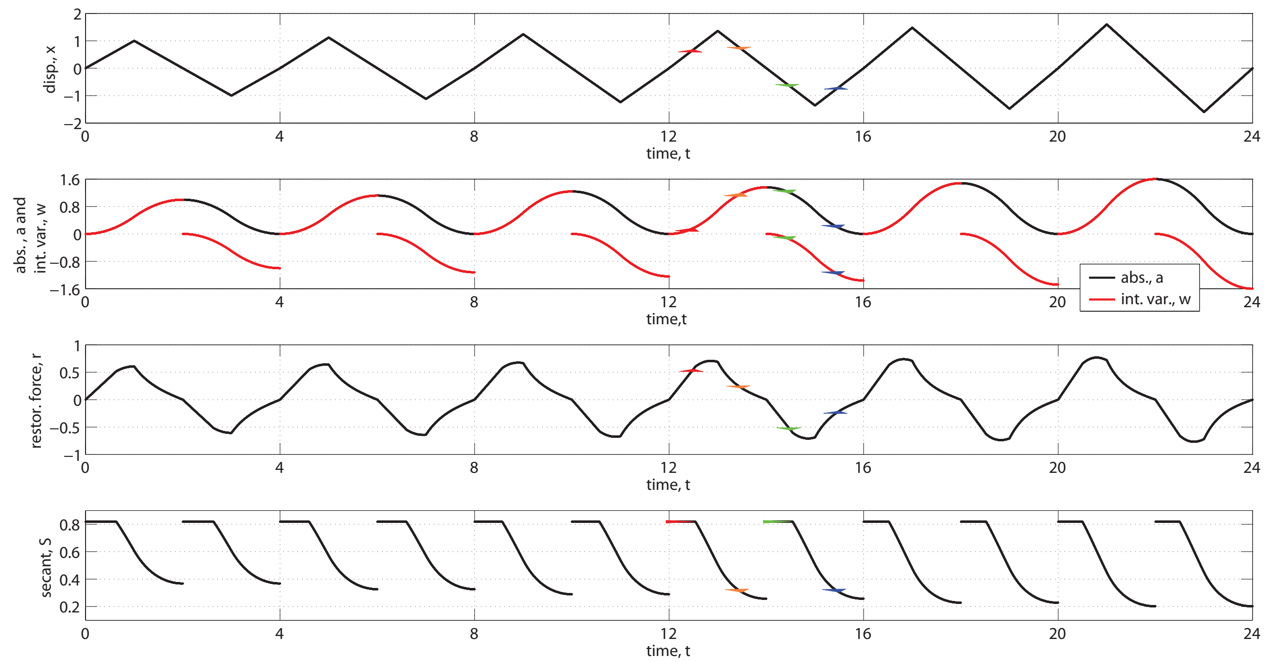

Fig. 23 Behaviors and inner workings of the proposed qualitative system model under multiple cycles of amplitude modulated sawtooth excitation - in terms of time histories - in contrast to those in Fig. 20.

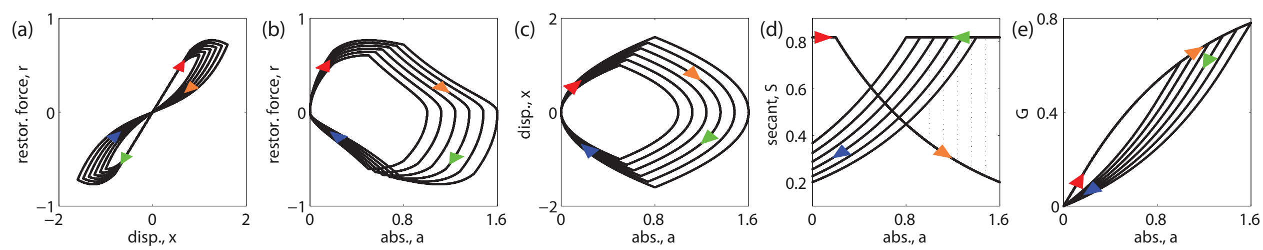

Fig. 24 Behaviors and inner workings of the proposed qualitative system model under multiple cycles of amplitude modulated sawtooth excitation - in terms of hysteretic loops - in contrast to those in Fig. 21 and more.

itive and meminductive theories with Di Ventra and Pershin in Di Ventra et al (2009). Table 2 summarizes the results of transplanting these theories to the field of engineering mechanics by following the lead of Oster and Auslander (1973) and Jeltsema and Scherpen (2009). Many examples of memristors and memcapacitive systems, called memdashpots, were found in the literature; however the same could not be said of memcapacitors or memcapacitive systems, called mem-springs. Mathematical parallelisms between mem-dashpots and mem-springs were recognized and exploited, but physical differences and the newness of mem-springs led to the realization that these newer models deserve deeper study, in part because of a little-studied quantity called absement which allows mem-spring models to display hysteretic response in great abundance. However it is nontrivial to devise mem-spring models that, when subjected to arbitrary excitations, are passive. Even for periodic excitations, a switching mechanism was needed so that simulations with prototype mem-spring models could maintain passivity, as in Fig. 1. Moreover, the input-output equations for all mem-models in Table 2 are scalar, as is Hooke's law, which implies that embedding mem-models in continuum mechanics is a nontrivial task. The mathematical form of the stress-strain equations that arise from such considerations involve secant modulus rather than tangent modulus, so these inherently nonlinear models are partly algebraic (the input-output equation) and partly differential (the state equation). In other words, the stress-strain equations that emerge from generalizing a scalar mem-spring model would involve total stress and strain (not incremental relations as in plasticity). As Willam (2002) notes, different versions (algebraic, differential) of nonlinear elasticity alone (to say nothing of inelasticity) lead to constitutive formulations that display fundamental differences under triaxial conditions. Clearly these nonlinear constitutive models merit more study.

REFERENCES

ACI Committee 318 (2011) Building Code Requirements for Structural Concrete and Commentary. American Concrete Institute

Applied Technology Council (2001) Evaluation and improvement of inelastic seismic analysis procedures,phase ii work plan, www.atcouncil.org

Bellenger H, Duvel JP (2009) An analysis of tropical ocean diurnal warm layers. J Climate 22:3629–3646

Bernstein DS (ed) (2009) IEEE Control Systems Magazine, vol 29, IEEE Control Systems Society, IEEE

Caughey TK (1960a) Random excitation of a system with bilinear hysteresis. Journal of Applied Mechanics 27:649–652

Caughey TK (1960b) Sinusoidal excitation of a system with bilinear hysteresis. Journal of Applied Mechanics 27:640–643

Chang T, Jo SH, Kim KH, Sheridan P, Gaba S, Lu W (2011) Synaptic behaviors and modeling of a metal oxide memristive device. Appl Phys 102:857–863

Christopoulos C, Tremblay R, Kim HJ, Lacerte M (2008) Self-centering energy dissipative bracing system for the seismic resistance of structures: Development and validation. ASCE Journal of Structural Engineering 134(1):96–107

Chua LO (1971) Memrister - the missing circuit element. IEEE Transactions on Circuit Theory CT-18(5):507–519

Chua LO, Kang SM (1976) Memristive devices and systems. In: Proceedings of the IEEE, vol 64, pp 209–223

Damic V, Cohodar M (2006) Bond graph based modelling and simulation of flexible robotic manipulators. In: Wolfgang Borutzky RZ Alessandra Orsoni (ed) Proceedings 20th European Conference on Modelling and Simulation

Di Ventra M, Pershin YV (2013) On the physical properties of memristive, memcapacitive, and meminductive systems. Nanotechnology 24(25), http://arxiv.org/abs/1302.7063

Di Ventra M, Pershin YV, Chua LO (2009) Circuit elements with memory: Memristors, memcapacitors, and meminductors. In: Proceedings of IEEE, vol 97, pp 1717–1724

Dolce M, Cardone D, Marnetto R (2000) Implementation and testing of passive control devices based on shape memory alloys. Earthquake Engineering and Structural Dynamics 29:945–968

Farrar CR, Worden K, Todd MD, Park G, Nichols J, Adams DE, Bement MT, Fairnholt K (2007) Nonlinear system identification for damage detection. Tech. Rep. LA-14353, Los Alamos National Laboratory

Ferri AA (1995) Friction damping and isolation systems. ASME Journal of Mechanical Design 117(B):196–206

Georgiou PS, Yaliraki SN, Drakakis EM, Barahona M (2012) Quantitative measure of hysteresis for memristor through explicit dynamics. Proceedings of The Royal Society A Mathematical Physical & Engineering Science 468:1–20

Guckenheimer J, Holmes P (1983) Nonlinear Oscillators, Dynamical Systems, and Bifurcations of Vector Fields, Applied Mathematical Sciences, vol 42. Springer-Verlag, New York

Hogan N, Breedveld PC (2002) The Mechatronics Handbook, CRC Press, chap 15. The Physical Basis of Analogies in Physical System Models

Ilbeigi S, Jahanpour J, Farshidianfar A (2012) A novel scheme for nonlinear displacement-dependent dampers. Nonlinear Dynamics 70:421–434

Inman DJ (1994) Engineering Vibration. Prentice Hall

Jeltsema D (2012) Memory elements: A paradigm shift in lagrangian modeling of electrical circuits. In: Proc. MathMod Conference, Vienna

Jeltsema D, Dòria-Cerezo A (2010) Mechanical memory elements: Modeling of systems with position-dependent mass revisited. In: 49th IEEE Conference on Decision and Control, IEEE, Atlanta, GA, pp 3511–3516

Jeltsema D, Scherpen JMA (2009) Multidomain modeling of nonlinear networks and systems: Energy- and power-based perspectives. IEEE Control Systems Magazine pp 28–59

Jennings PC (1964) Periodic response of a general yielding structure. Journal of the Engineering Mechanics Division, Proceedings of the American Society of Civil Engineers 90(EM2):131–166

Kalmár-Nagy T, Shekhawat A (2009) Nonlinear dynamics of oscillators with bilinear hysteresis and sinusoidal excitation. Physica D 238:1768–1786

Madhekar SN, Jangid RS (2009) Variable dampers for earthquake protection of benchmark highway bridges. Smart Materials and Structures 18:1–18

Masri SF, Caughey TK (1979) A nonparametric identification technique for nonlinear dynamic problems. Journal of Applied Mechanics 46:433–447

Nayfeh AH, Mook DT (1995) Nonlinear Oscillations. Wiley-VCH

Ogata K (2004) System Dynamics, 4th edn. Pearson Prentice Hall

Oster GF, Auslander DM (1973) The memristor: A new bond graph element. ASME Journal of Dynamic Systems, Measurement, and Control 94(3):249–252

Paynter HM (1961) Analysis and Design of Engineering Systems: Class Notes for M.I.T. Course 2.751. M.I.T. Press

Paytner HM (2000) The gestation and birth of bond graphs. http://www.me.utexas.edu/~longoria/paynter/hmp/Bondgraphs.html

Priestley MJN, Grant DN (2010) Viscous damping and seismic design and analysis. Journal of Earthquake Engineer-

ing 9(2):229–255
Ricles JM, Sause R, Peng SW, Lu LW (2002) Experimental evaluation of earthquake resistant posttensioned steel connections. ASCE Journal of Structural Engineering 128(7):850–859
Rosenberg RC, Karnopp DC (1983) Introduction to Physical System Dynamics. McGraw-Hill Series in Mechanical Engineering, McGraw-Hill, Inc.
Santos FP, Cismaşiu C (2007) Shape memory alloys in structural vibration control. In: Experimental Vibration Analysis for Civil Engineering Structures (EVACES'07), FEUP, Porto, Portugal
Scruggs JT, Gavin HP (2010) The Control Handbook, 2nd edn, CRC Press, chap Earthquake Response Control for Civil Structures
Sivaselvan MV, Reinhorn AM (2000) Hysteretic models for deteriorating inelastic structures. ASCE Journal of Engineering Mechanics 126(6):633–640
Sozen MA (1974) Hysteresis in Structural Elements, ASME, New York, NY, pp 63–98
Strogatz SH (1994) Nonlinear Dynamics and Chaos with Applications to Physics, Biology, Chemistry, and Engineering. Studies in Nonlinearity, Westview Press
Strukov D (2011) Memristors & their applications
Strukov DB, Snider GS, Stewart DR, Williams RS (2008) The missing memristor found. Nature 453:80–83
Talasila V, Golo G, van der Schaft AJ (2002) The wave equation as a port-hamiltonian system, and a finite dimensional approximation. http://doc.utwente.nl/69144/1/1182.pdf
Vaz A, Maini AK (2009) Modeling of soft materials: Integrating bond graphs with finite element analysis. In: 14th National Conference on Machines and Mechanisms (NaCoMM09), NIT, Burgapur, India, pp 247–252
Visintin A (1994) Differential Models of Hysteresis. Springer
Willam KJ (2002) Encyclopedia of Physics Science & Technology, vol 3, 3rd edn, Academic Press, chap Constitutive Models for Engineering Materials, pp 603–633
Williams RS (2008) How we found the missing memristor. IEEE Spectrum 45(12):28–35
Wright JP, Pei JS (2012) Solving dynamical systems involving piecewise restoring force using state event location. ASCE Journal of Engineering Mechanics 138(8):997–1020
Zhu S, Zhang Y (2007) A thermomechanical constitutive model for superelastic sma wire with strain-rate dependence. Smart Mater Struct 16:1696–1707

NOTATION

$\dot{x}$	velocity
x	displacement
a	absement, first time integral of displacement, x
σ	stress
ε	strain
ε_t	strain rate
α	strain absement
$\dot{r}$	the first time derivative of r
r	resisting force or characteristic force of an element
p	general momentum, the first time integral of r
ρ	the first time integral of p
$\mathbf{y}$	state variables, see Tables 2 and 3
$\mathbf{z}$	state variables in Table 9
w	internal state or intermediate variable in Sections 4 and 5
u	driving force, see Eq. (1), Fig. 25 and Table 9
M	incremental memristance following Chua (1971)
W	incremental memdunctance following Chua (1971)
G	See Table 2
F	See Table 2
$\mathbf{g}$	See Table 2
$\mathbf{f}$	See Table 2
e	effort
f	flow
D	secant damping, See Table 3 and Fig. 15
S	secant stiffness, see Table 3 and Fig. 15
K	tangent stiffness, see Property 4
P	power, See Table 3
U	energy, see Table 3
a_0	See Section 3.3, especially Table 4
i	current
v	voltage
q	charge
φ, ϕ	flux

7 ACKNOWLEDGEMENTS

Part of this work was initiated during the first author's sabbatical leave, partially funded by NSF CMMI 0626401 with Program Officer, Dr. S.C. Liu; she would like to thank Professor Jim Beck and Professor Jeff Scruggs for their hospitality. The authors would like to thank Professor Jim Beck for providing us with Eq. (48) and helpful comments to earlier drafts, Professor Jeff Scruggs, Professor Dennis Bernstein, and Dr. Giovanni Paziena for referring us to the following references, respectively, Ogata (2004), Jeltsema and Scherpen (2009) and Strukov (2011). The first author wishes to thank Professor Shirley Dyke for assistance in finding data for the PC4 specimen in Ricles et al (2002).

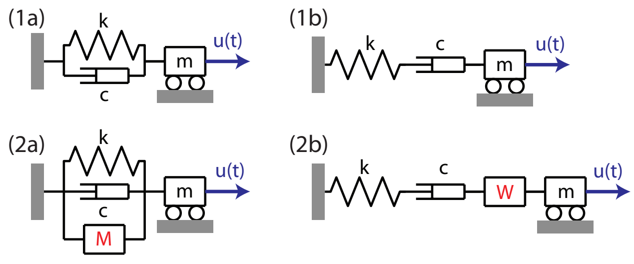

Fig. 25 (1a) A Kelvin model connected in series with a mass; (1b) a Maxwell model connected in series with a mass; (2a) a Kelvin model connected with a memristor in parallel and then connected in series with a mass, and (2b) a Maxwell model connected with a memristor in series and then connected in series with a mass. Each is subject to a prescribed force $u(t)$.

A Appendix for Section 2

Table 8 lists various definitions of the memristor and the publications from which they were taken. First, these seemingly different definitions are indeed all consistent once notational differences are taken into account. Next, they are for either a general or a specific electrical system. Last, they distinguish a flow- from an effort-controlled electrical device. For electrical systems, charge- or current-controlled are aliases for flow-controlled, while flux-, voltage-, or impulse-controlled are aliases for effort-controlled.

Figure 25 depicts some simple situations where the necessity to contrast flow- and effort-controlled mechanical systems becomes evident. After all, basic elements like springs, dampers, or memristors are made to be used repetitively and in a well-organized manner in order to form a "system" that models a complex real-world device or structure. For translational mechanics, the connectivity of these basic elements can be reduced to either parallel or serial connections, the roots of the concepts of flow- and effort-controlled systems.

Figures 25 (1a) and (1b) show the Kelvin and Maxwell models, each connected in series with a mass. Jeltsema and Scherpen (2009) reveal the duality between these flow- and effort-controlled systems, expressed in terms of integro-differential equations. In a flow-controlled device, the natural state variables are displacement x and velocity $\dot{x}$. These state variables should be solved (or calculated) first by integrating the differential equation based on force equilibrium. In contrast, in an effort-controlled device, the natural state variables are momentum p and restoring force r, where momentum is the time integral of restoring force. These state variables should be solved (or calculated) first from the equation based on deformation compatibility.

These two linear time-invariant flow- and effort-controlled systems may be extended by introducing a new element – such as the memristor (nonlinear time-invariant) – as shown in Fig. 25 (2a) and (2b). Table 9 presents the state variables and state equations for the corresponding models in Fig. 25, where $u(t)$ is an applied force as in Eq. (1). For systems in general, the constitutive relations of all components – either elements or systems – need to be "assembled" in accord with the connectivity of the components. Absent other important details, the need for two different mathematical expressions for the same memristor to fit into these two different systems may be seen clearly. In other words, when doing computations, we may need to deal with either a flow-controlled memristor or an effort-controlled memristor, depending on the element or system connectivity.

Table 10 lists expressions that are analogous to the set of (i, v) plots in Strukov (2011) under the title of "Curious Lay Person's Viewgraph - II", plus one more for the memcapacitor. Table 10 also illustrates the underlying mathematical parallelism in the case of sinusoidal excitation.

Table 13 Secant stiffness $S(a, x)$ used in simple mem-spring models $r = S(a, x)x$ in Section 3.4.

Fig. ID	$S(a, x)$
10(a)	$\mathrm{sgn}\,(x)\cos\left(\frac{\pi a}{2a_0}\right)+2$
10(b)	$-\mathrm{sgn}\,(x)\cos\left(\frac{\pi a}{2a_0}\right)+2$
11(b)	$\frac{1-\mathrm{sgn}((a-a_0)x)}{2}\times 3+\frac{1+\mathrm{sgn}((a-a_0)x)}{2}\times 1$
26(a) & 27(a)	$\frac{1-\mathrm{sgn}((a-a_0)x)}{2}\left(1+\frac{2}{a_0^2}(a-a_0)^2\right)+$ $\frac{1+\mathrm{sgn}((a-a_0)x)}{2}\left(1+\frac{2}{a_0^6}(a-a_0)^6\right)$
26(b) & 27(b)	$\frac{1-\mathrm{sgn}((a-a_0)x)}{2}\left(3-\frac{2}{a_0}\left(a-\frac{1-\mathrm{sgn}(x)}{2}2a_0\right)^2\right)+$ $\frac{1+\mathrm{sgn}((a-a_0)x)}{2}\left(1+\frac{2}{a_0^6}(a-a_0)^6\right)$

The proof to Remark 4 is given below. The equation of motion corresponding to Fig. 25(2a) is:

$$m\ddot{x}+kx=u-[c+M(x)]\,\dot{x},\ \text{with}\ x(0)=x_0, \dot{x}(0)=\dot{x}_0 \quad (43)$$

Assume free vibration; i.e., $u = 0$. Multiply both sides of Eq. (43) by $\dot{x}(t)$. Note that

$$(m\ddot{x}+kx)\,\dot{x}=\frac{d}{dt}E(t) \quad (44)$$

where $E(t)=\frac{1}{2}m\dot{x}^2+\frac{1}{2}kx^2$. Multiply this equation by dt and integrate from $t = 0$ to $t = T$ to obtain $E(T) = E(0) - \Delta(T)$, where

$$\Delta(T)=\int_0^T [c+M(x)]\,\dot{x}^2 dt \quad (45)$$

is a dissipation function. If $c + M(x) \geq 0$, $\forall x(t)$, then $\Delta(T) \geq 0$. Thus, $M(x) \geq -c$ is sufficient for passivity (i.e., no produced energy).

B Appendix for Section 3

See Tables 12 and 13 for some models used in Sections 3.3 and 3.4, respectively:

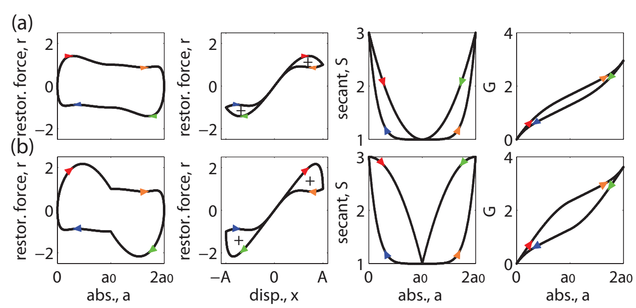

Fig. 26 Two system models (see Table 13) illustrate the behavior of (x, r) at $x = 0$ and the impact of (a) Situation (1), and (b) Situation (2) to the tangent stiffness of (x, r); $x(t) = A\sin(\omega t)$ with $A = 1$ and $\omega = 1$.

C Appendix for Section 4

C.1 Case studies from nano-field

Tables 14 and 15 give an overview of all these case studies.

Table 8 Many faces of mathematical expressions for the memristor. All notations in this table follow those in the original publications. Note: φ is the same as ϕ.

In Device of	Algebraic Form	Differential Form
"charge-controlled" (Chua (1971))		$v(t) = M(q(t))i(t), M(q) = \frac{d\varphi(q)}{dq}$
"charge-controlled" (Oster and Auslander (1973))	$p = G(q)$	$\dot{p} = G'(q)\dot{q} \Longrightarrow e = M(q)f$
"charge-controlled" (Jeltsema and Scherpen (2009))	$\phi = \hat{\phi}(q)$	$V = M(q)I$
"flux-controlled" (Chua (1971))		$i(t) = W(\varphi(t))v(t), W(\varphi) = \frac{dq(\varphi)}{d\varphi}$
"impulse-controlled" (Oster and Auslander (1973))	$q = F(p)$	$\dot{q} = F'(p)\dot{p} \Longrightarrow f = W(p)e$
"flux-controlled" (Jeltsema and Scherpen (2009))	$q = \hat{q}(\phi)$	$I = W(\phi)V$

Table 9 Summary of possible state variables and equations for all cases in Fig. 25.

Flow-Controlled	Force-Controlled
Fig. 25(1a)	Fig. 25(1b)
$\mathbf{z} = \begin{bmatrix} x \\ \dot{x} \end{bmatrix}$	$\mathbf{z} = \begin{bmatrix} p \\ r \end{bmatrix}$
$\dot{\mathbf{z}} = \begin{bmatrix} \dot{x} \\ \ddot{x} \end{bmatrix} = \begin{bmatrix} 0 & 1 \\ -\frac{k}{m} & -\frac{c}{m} \end{bmatrix} \underbrace{\begin{bmatrix} x \\ \dot{x} \end{bmatrix}}_{\mathbf{z}} + \begin{bmatrix} 0 \\ \frac{1}{m} \end{bmatrix} u$	$\dot{\mathbf{z}} = \begin{bmatrix} r \\ \dot{r} \end{bmatrix} = \begin{bmatrix} 0 & 1 \\ -\frac{k}{m} & -\frac{k}{c} \end{bmatrix} \underbrace{\begin{bmatrix} p \\ r \end{bmatrix}}_{\mathbf{z}} + \begin{bmatrix} 0 \\ \frac{k}{m} \end{bmatrix} \int u dt$
Fig. 25(2a)	Fig. 25(2b)
$\mathbf{z} = \begin{bmatrix} x \\ \dot{x} \end{bmatrix} \triangleq \begin{bmatrix} z_1 \\ z_2 \end{bmatrix}$	$\mathbf{z} = \begin{bmatrix} p \\ r \end{bmatrix} \triangleq \begin{bmatrix} z_1 \\ z_2 \end{bmatrix}$
$\dot{\mathbf{z}} = \begin{bmatrix} z_2 \\ -\frac{1}{m}\left(kz_1 + cz_2 + M(z_1)z_2\right) + \frac{1}{m}u \end{bmatrix}$	$\dot{\mathbf{z}} = \begin{bmatrix} z_2 \\ -k\left(\frac{1}{m}z_1 + \frac{1}{c}z_2 + W(z_1)z_2\right) + \frac{k}{m}\int u dt \end{bmatrix}$

Table 10 Periodic solution for spring and memcapacitor subject to †$x(t) = A\sin(\omega t)$, and for mass, dashpot and memristor subect to ‡$\dot{x}(t) = A\sin(\omega t)$. ♯ Other damper equations may be used.

Element	r	Expression for r	Signature Plot
Spring†	$r = kx$	$kA\sin(\omega t)$	an ellipse $\frac{\dot{x}^2}{(A\omega)^2} + \frac{r^2}{(kA)^2} = 1$ in the ($\dot{x}$, r) plane
Memcapacitor†	$r = M(a)x$	$M\left(\frac{A}{\omega} - \frac{A}{\omega}\cos(\omega t)\right) \cdot A\sin(\omega t)$	"bow tie" in the (x, r) plane
Mass‡	$r = m\ddot{x}$	$mA\omega\cos(\omega t)$	an ellipse $\frac{\dot{x}^2}{A^2} + \frac{r^2}{(mA\omega)^2} = 1$ in the ($\dot{x}$, r) plane
Dashpot‡, ♯	$r = c\dot{x}$	$cA\sin(\omega t)$	one-to-one mapping in the ($\dot{x}$, r) plane
Memristor‡	$r = M(x)\dot{x}$	$M\left(\frac{A}{\omega} - \frac{A}{\omega}\cos(\omega t)\right) \cdot A\sin(\omega t)$	"bow tie" in the ($\dot{x}$, r) plane (Williams (2008))

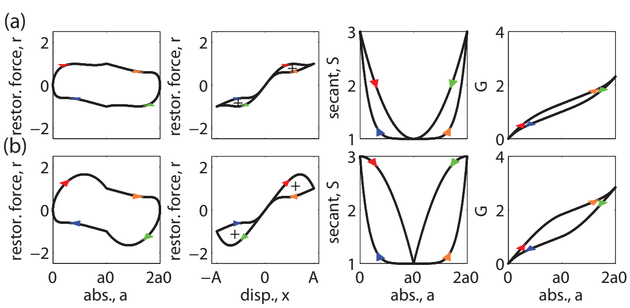

Fig. 27 The same system models as in Fig. 26 (see Table 13) but subject to $x(t) = \frac{4A}{T}\left(t - \frac{T}{2}\left\lfloor\frac{2t}{T} + \frac{1}{2}\right\rfloor\right)(-1)^{\lfloor\frac{2t}{T}+\frac{1}{2}\rfloor}$, with $a(0) = 0$, $T = \frac{2\pi}{\omega}$, $A = 1$, and $\omega = 1$. This is to illustrate the behavior of (x, r) at $x = 0$ and the impact of (a) Situation (1), and (b) Situation (2) to the tangent stiffness of (x, r).

C.2 Understanding case study #3

To see that $W = \frac{i(t)}{v(t)}$ is a bivariate function of $v(t)$ and $\phi(t)$, note that $i(t)$, defined by Eq. (58), is a bivariate function of $w(t)$ and $v(t)$. Applying the fundamental existence-uniqueness theorem for ODEs (e.g., in Guckenheimer and Holmes (1983)) to Eq. (57), the solution exists and is unique on an open set for v; i.e., (w, ϕ) is one to one (since the hyperbolic sine in Eq. (57) is analytic and thus satisfies the Lipschitz condition). Hence, $W = f(w(\phi), v) = g(\phi, v)$.

Table 14 Three case studies on nano-devices selected as case studies herein with the equation or page numbers appeared in these papers.

Case Study	Reference	State Eqs.	I/O Eq.
#1	Strukov et al (2008)	Eq. (6)	Eq. (5)
#2	Strukov (2011)	pp. 17	pp. 15
#3	Chang et al (2011)	Eq. (5)	Eq. (4)

Hereafter consider only prescribed piecewise linear $v(t)$ as in Chang et al (2011). Assume $v(t) = bt + c$ for a generic section of the excitation and proceed as follows:

$$\frac{d\phi}{dv} = \frac{\dot{\phi}}{\dot{v}} = \frac{v(t)}{b} \tag{59}$$

leading to the following piecewise relation for the phase plot (v, ϕ):

$$\phi(t) = \frac{v^2(t)}{2b} + \phi_0 \Longrightarrow v(t) = \pm\sqrt{2b(\phi(t) - \phi_0)} \tag{60}$$

Table 11 Examples of mem-dashpots.

ID	Application and Governing Eq.
1.	The Van der Pol oscillator and Liénard equation contain mem-dashpots. The Van der Pol oscillator can be viewed as a mem-dashpot connected in parallel with a linear dashpot and a linear spring before connecting in series with a mass, as illustrated in Fig. 25(2a): $\ddot{x} - \varepsilon[1-x^2]\dot{x} + x = 0, \text{ with } \varepsilon > 0 \implies \underbrace{\ddot{x}}_{\text{unit mass}} \underbrace{-\varepsilon\dot{x}}_{\text{classical dashpot}} + \underbrace{\varepsilon x^2\dot{x}}_{\text{mem-dashpot}} + \underbrace{x}_{\text{classical spring}} = 0$ (46) A more general expression for a mem-dashpot in a flow-controlled mechanical system is the term $D(x)\dot{x}$ in the Liénard equation: $\underbrace{\ddot{x}}_{\text{unit mass}} + \underbrace{D(x)\dot{x}}_{\text{mem-dashpot}} + \underbrace{f(x)}_{\text{nonlinear spring}} = 0$ (47) The Liénard equation, which includes the Van der Pol oscillator, is one of the most theoretically studied nonlinear dynamics equations (e.g., Guckenheimer and Holmes (1983); Strogatz (1994); Nayfeh and Mook (1995)).
2.	Displacement-dependent dampers, which have been investigated for earthquake mitigation (Ferri (1995); Priestley and Grant (2010)), are mem-dashpots. A general form is: $D(x) = \sum_{n=1}^{\infty} \alpha_n \lvert x\rvert^n, \;\; \alpha_n \geq 0$ (48) where the use of the absolute function and the requirement of non-negativity of α_n are to ensure passivity of the memristor (Remark 4). Ilbeigi et al (2012) studied nonlinear displacement-dependent dampers of the type: $D(x) = \lambda \left[\mu^2 \left(\frac{1}{1-\beta x^{(\frac{1}{s})}}\right)^2 - 1\right]^2$ (49) where $\lambda > 0$ satisfies the passivity property, Remark 4, (μ, β and s are other design parameters). This formula is approximated using Taylor series expansion in Ilbeigi et al (2012), resulting in two other damper formulas as follows: $D(x) = \alpha_1 + \alpha_2\lvert x\rvert^{\frac{1}{s}} + \alpha_3\lvert x\rvert^{\frac{2}{s}} + \alpha_4\lvert x\rvert^{\frac{3}{s}} + \alpha_5\lvert x\rvert^{\frac{4}{s}}$ (50) $D(x) = \alpha_1 + \alpha_2 x^2 + \alpha_3 x^4 + \alpha_4 x^6 + \alpha_5 x^8$ (51) Each of these can be considered a linear viscous damper connected with memristors (mem-dashpots) in series. The passivity conditions α's ≥ 0 are satisfied in Ilbeigi et al (2012) but not mentioned.
3.	Variable dampers have been studied for earthquake mitigation as well. Unlike the displacement-dependent dampers discussed above, they are not memristors but they are memristive systems. For example, setting $\mathbf{y} = x$, the two-step viscous damping in Madhekar and Jangid (2009) is of the form: $r = \underbrace{\left[\frac{1}{2}\left(1+\text{sgn}\left(x\dot{x}\right)\right)c_{d_1} + \frac{1}{2}\left(1-\text{sgn}\left(x\dot{x}\right)\right)c_{d_2}\right]}_{D(\mathbf{y},\dot{x})}\dot{x}$ (52) where c_{d_1} and c_{d_2} are two different viscosity values. This is an input-output equation of a time-invariant flow-controlled mem-dashpot as in Table 3; also see the two ($\dot{x}$, r) plots with prominent zero-crossing feature in Madhekar and Jangid (2009).

The general solution of Eq. (57) with $v(t) = bt + c$ is:

$$w(t) = w(t_0) + \frac{2\lambda}{\eta b}\left[\cosh(\eta v(t)) - \cosh(\eta b t_0 + \eta c)\right] \tag{61}$$

$$\overset{\text{Eq. (60)}}{=} w(t_0) + \frac{2\lambda}{\eta b}\left[\cosh\left(\pm\eta\sqrt{2b\left(\phi(t)-\phi_0\right)}\right) - \cosh(\eta b t_0 + \eta c)\right] \tag{62}$$

where the sign $\pm$ remains the same within each piece as before. Clearly, (w, ϕ) is a one-to-one mapping within each piece of the solution curve separated by the time events. Given that cosh is an even function, the first and third quadrants in (v, i) share the same (w, ϕ). These can be verified in Fig. 28.

Substituting Eqs. (61) to (58), it can be seen that, for a pair of v and $-v$, the absolute values of their i differ, so do their q and W values - as

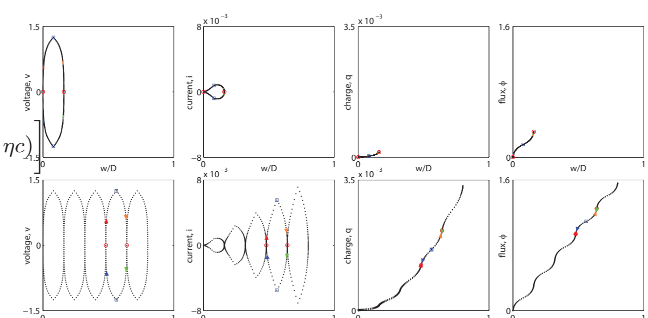

Fig. 28 More insights in terms of $\frac{w}{D}$ to understand Chang et al (2011)'s Fig. 5a and Fig. 5b.

Table 12 Secant stiffness $S(a)$ used in simple mem-spring models $r = S(a)x$ in Section 3.3.

Fig. ID	$S(a)$	Differentiability Classification
3(a)	$(a-a_0)^2+2$	$\mathcal{C}^\omega$ (analytic), quadratic function of a
3(b)	$\lvert a-a_0\rvert+2=\frac{1-\text{sgn}(a-a_0)}{2}\left(3-\frac{a}{a_0}\right)+\frac{1+\text{sgn}(a-a_0)}{2}\left(2+\frac{a-a_0}{a_0}\right)$	$\mathcal{C}^0$, continuous at a_0, piecewise linear
4(a) & 5(a)	$\cos\left(\frac{\pi a}{2a_0}\right)+2$	$\mathcal{C}^\omega$, analytic for all a
4(b) & 5(b)	$-\cos\left(\frac{\pi a}{2a_0}\right)+2$	$\mathcal{C}^\omega$, analytic for all a
6(a) & (b)	$\frac{1-\text{sgn}(a-a_0)}{2}\left[-\sin\left(\frac{\pi a}{2a_0}\right)+3\right]+\frac{1+\text{sgn}(a-a_0)}{2}\left[\sin\left(\frac{\pi a}{2a_0}\right)+1\right]$	$\mathcal{C}^1$, differentiable at a_0, piecewise analytic
7(a) & (b)	$\frac{1-\text{sgn}(a-a_0)}{2}\left(3-\frac{5a}{3a_0}\right)+\frac{1+\text{sgn}(a-a_0)}{2}\left(\frac{4}{3}-\frac{a-a_0}{3a_0}\right)$	$\mathcal{C}^0$, continuous at a_0, piecewise linear
8(a) & (b)	$\frac{1-\text{sgn}(a-a_0)}{2}\left[-\sin\left(\frac{\pi a}{2a_0}\right)+3\right]+\frac{1+\text{sgn}(a-a_0)}{2}\sin\left(\frac{\pi a}{2a_0}\right)$	$\mathcal{C}^{-1}$, integrable at a_0, piecewise analytic
11(a)	$\frac{1-\text{sgn}(a-a_0)}{2}\times 3+\frac{1+\text{sgn}(a-a_0)}{2}\times 1$	$\mathcal{C}^{-1}$, integrable at a_0, piecewise constant

Table 15 Case studies: Both the state and input-output equations are from the original papers where they are cited from.

ID	State and Input-Output Eqs. and Inter. Var.
1	Equations (6) and (5) from Strukov et al (2008) are the state and input-output equations to produce Fig. 2 in that paper: State Eq.: $\frac{dw}{dt}=\mu_V\frac{R_{ON}}{D}i$ (53) I/O Eq.: $v=\left(R_{ON}\frac{w}{D}+R_{OFF}\left(1-\frac{w}{D}\right)\right)i$ (54) where $v(t)=v_0\sin(\omega_0 t)$ and $v(t)=v_0\sin^2(\omega_0 t)$ for Fig. 2b and 2c, respectively, with $v_0=10$, and $\omega_0=10\pi$ - differing from Strukov et al (2008), where v_0 and ω of being 1 and 200π, respectively. In addition, $\frac{R_{OFF}}{R_{ON}}=160$ and $\frac{R_{OFF}}{R_{ON}}=380$ for Fig. 2b and 2c, respectively, $R_{ON}=100$, $\frac{D^2}{\mu_V}=0.01$, and $\frac{w}{D}\lvert_{t=0}=0.1$.
2	Strukov et al (2008) points that Chua does not anticipate w being bounded by 0 and D. A term called "window function" is used to simulate nonlinear drift when w approaches 0 and D. The expression for the term, unfortunately, has a typo. The correct one is given in Strukov (2011): State Eq.: $\frac{dw}{dt}=\mu_V\frac{R_{ON}}{D}i\frac{w}{D}\left(1-\frac{w}{D}\right)$ (55) I/O Eq.: $v=\left(R_{ON}\frac{w}{D}+R_{OFF}\left(1-\frac{w}{D}\right)\right)i$ (56) where $\frac{R_{OFF}}{R_{ON}}=50$, $R_{ON}=100$, $\frac{D^2}{\mu_V}=0.01$, and $\frac{w}{D}\lvert_{t=0}=0.001$ assumed by the authors - not being zero as $w\in(0,D)$ on pp. 17 of Strukov (2011). To reproduce the response given on pp. 17 in Strukov (2011), the authors were able to follow the specified frequency but not amplitude.
3	From Chang et al (2011): State Eq.: $\frac{dw}{dt}=2\lambda\sinh(\eta v)$ (57) I/O Eq.: $i=\left(1-\frac{w}{D}\right)\alpha\left[1-e^{-\beta v}\right]+\frac{w}{D}\gamma\sinh(\delta v)$ (58) where $\lambda=4.5$, $\eta=4$, $\alpha=0.5\times10^{-6}$, $\beta=0.5$, $\gamma=4\times10^{-6}$, and $\delta=2$. $D=412.5$ was obtained by trial-and-error in this study with $\frac{w}{D}$ as given in Eq. (58) (instead of Eq. (4) in Chang et al (2011) which gives a wrong range for i).

stated in the caption for Fig. 19. Indeed, this system is not a memristor; rather it is a memristive system.

In fact, the pair of $\dot{w}$ and v defined in Eq. (57) represents a relationship in a nonlinear resister with $\dot{w}$ and w corresponding to current and charge, respectively. Having said this, (w, ϕ) must be a one-to-one mapping as stated above and illustrated in Fig. 28. Alternatively (and at the risk of unnecessary length), the one-to-one'ness and inflection points on (w, ϕ) shown in Fig. 28 can be understood as follows:

$$\frac{dw}{d\phi}=\frac{\dot{w}}{\dot{\phi}}=\frac{2\lambda\sinh(\eta v)}{v} \tag{63}$$

For all $v(t)$, $\frac{dw}{d\phi}>0$, which explains the monotonic (w, ϕ); i.e., (w, ϕ) is one-to-one for all t. Furthermore, the continuity of $\sinh$ can be used to explain the continuity of (w, ϕ) even when $v(t)$ is only $\mathcal{C}^0$ continuous.

D Appendix for Section 5

A prototype mem-spring model for SMA wire is given as herein. While the models in Figs. 26 and 27 could be candidates for SMA wire in tension (e,g., those in Dolce et al (2000)), there is a useful methodology for establishing a memcapacitor model for any individual set of SMA wire data under a clearly defined excitation - if we adopt the philosophy of Section 4.6 by paying attention to time-varying secants. For the piecewise-defined displacement in Eqs. (13) to (16), this methodology is illustrated in Fig. 29 and explained in the next two paragraphs.

The mathematical expressions involved in modeling - for the example illustrated in Fig. 29 - are given as follows:

$$r_1(x) \Rightarrow s_1(x) = \frac{r_1(x)}{x} = s_1(h_1(a)) = S_1(a) \tag{64}$$

$$r_2(x) \Rightarrow s_2(x) = \frac{r_2(x)}{x} = s_2(h_2(a)) = S_2(a) \tag{65}$$

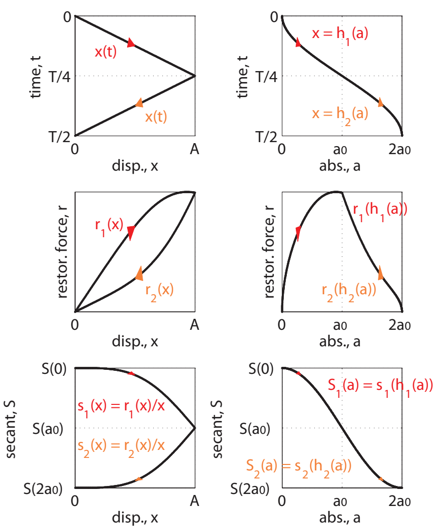

Fig. 29 Illustrations of the procedure of developing a memcapacitor model by using an arbitrary set of SMA wire under a piecewise linear displacement as in Eqs. (13) to (16).

To clearly demonstrate this modeling method, Fig. 9 presented previously is utilized again. The restoring force vs. displacement plot in the first quadrant is examined first. As shown in Fig. 30, the model parameters x_1, r_1, and x_2 are to be given in advance. Others can be conveniently obtained from geometry: $r_2 = R - \frac{A-x_2}{x_1} r_1$ where R is the restoring force corresponding to A, $x_3 = x_2 - (A - x_1)$; $r_3 = \frac{x_3}{x_1} r_1$. The corresponding absement values are: $a_1 = \frac{T}{8A} x_1^2$; $a_2 = 2a_0 - \frac{T}{8A} x_2^2$, and $a_3 = 2a_0 - \frac{T}{8A} x_3^2$. By varying the values of x_1, r_1 and x_2, a set of these sub-models are obtained. In all these sub-models, applying Eqs. (64) and (65) but considering a total of five pieces that characterize an experimental restoring force vs. displacement plot, we have the following equations to define $S(a)$ in a piecewise manner:

$$S_1(a) = \frac{r_1}{x_1},$$
$$a \in [0, a_1], \quad \text{red lines in Fig. 30} \tag{66}$$

$$S_2(a) = \left(r_1 - \frac{x_1}{A - x_1}(R - r_1)\right)\sqrt{\frac{T}{8Aa}} + \frac{R - r_1}{A - x_1},$$
$$a \in [a_1, a_0], \quad \text{orange lines in Fig. 30} \tag{67}$$

$$S_3(a) = \left(R - \frac{A}{x_1} r_1\right)\sqrt{\frac{T}{8A(2a_0 - a)}} + \frac{r_1}{x_1},$$
$$a \in [a_0, a_2], \quad \text{green lines in Fig. 30} \tag{68}$$

$$S_4(a) = \left(r_3 - \frac{x_3}{x_2 - x_3}(r_2 - r_3)\right)\sqrt{\frac{T}{8A(2a_0 - a)}} + \frac{r_2 - r_3}{x_2 - x_3},$$
$$a \in [a_2, a_3], \quad \text{blue lines in Fig. 30} \tag{69}$$

$$S_5(a) = \frac{r_1}{x_1},$$
$$a \in [a_3, 2a_0], \quad \text{black lines in Fig. 30} \tag{70}$$

After finishing modeling the first quadrant, the model in the third quadrant must be made “anti-symmetric with respect to the origin” following Di Ventra et al (2009) (see Section 3.4), which is conveniently carried out, say, using vector concatenation under MATLAB. Mathematically, this could be done using either of two approaches given in Sections 5.2 and 5.3. Data sets from other analytic or piecewise continuous displacements can be treated in a similar manner.

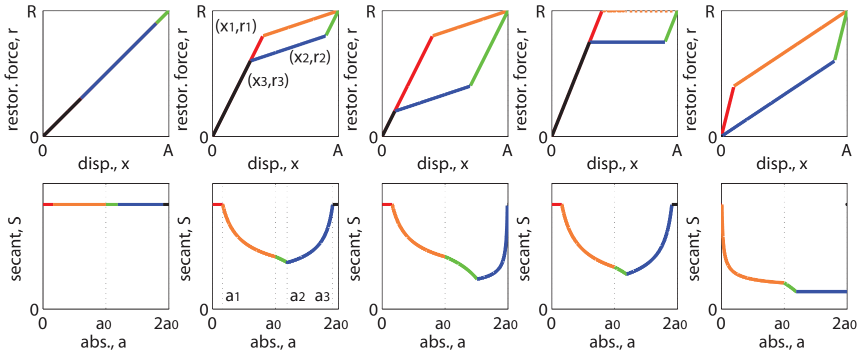

Fig. 30 To expand on Fig. 9, different variations in the hysteric loop in the first quadrant (subject to a piecewise linear displacement) and their corresponding models. The piecewise linear displacement is defined in Eqs. (13) to (16) with $a(0) = 0$, $A = 1$, and $\omega = 1$. Five sets of values are used for x_1, r_1 and x_2.